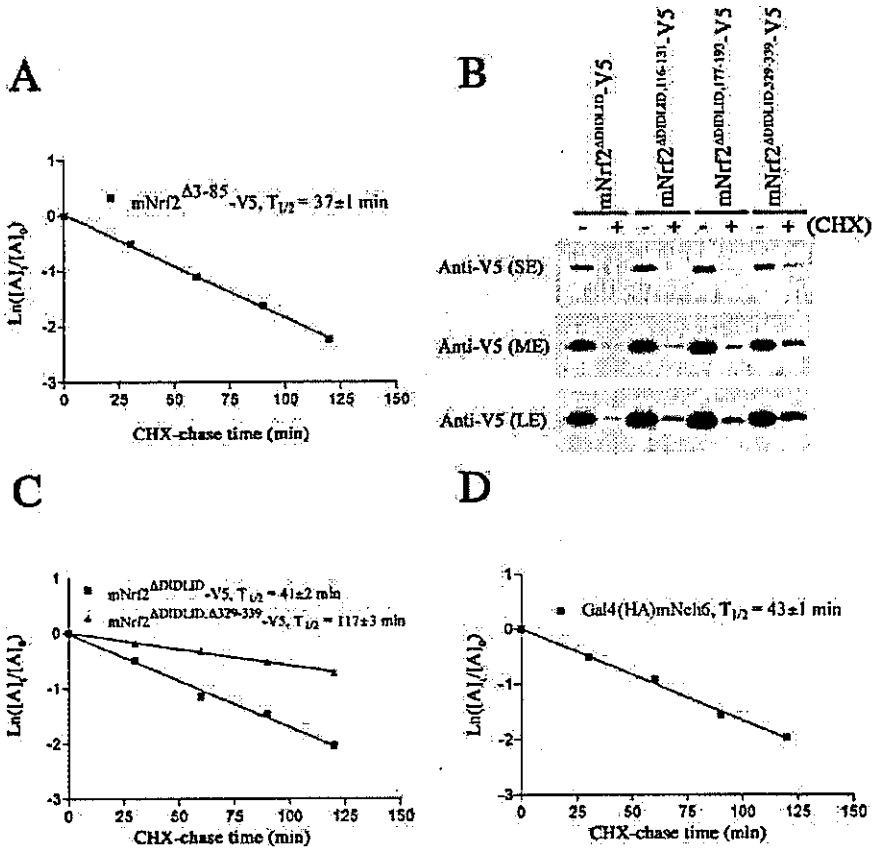

FIG. 7. **The Neh6 domain is a redox-insensitive degron.** *A*, COS1 cells in 60-mm dishes were transfected with 2 μg of a vector expressing mNrf2$^{\Delta 3-85}$-V5, 2 μg of pcDNA3.1/mKeap1, and 0.8 μg of pCMVβ-gal. 24 h after transfection, CHX was added to a final concentration of 40 μg/ml, and whole-cell lysates were prepared at different time points and probed with mouse anti-V5. The graph depicts the natural logarithm of the relative expression of mNrf2$^{\Delta 3-85}$-V5 as a function of CHX chase time (mean of two independent experiments). The best fit line and the derived half-life are depicted. *B*, COS1 cells in 60-mm dishes were transfected with 2 μg of vector expressing either of the four V5-tagged proteins indicated, 2 μg of pcDNA3.1/mKeap1, and 0.8 μg of pCMVβ-gal. 24 h later, cells were treated with either 0.1% (v/v) Me_2SO (−) or 40 μg/ml CHX (+) for 3 h before whole-cell lysates were prepared and probed with mouse anti-V5. *C* and *D*, COS1 cells in 60-mm dishes were transfected with 2 μg of pcDNA3.1/mKeap1, 0.8 μg of pCMVβ-gal, and 2 μg of vector expressing either one of the two indicated V5-tagged proteins (*C*) or Gal4(HA)mNeh6 protein (*D*). 24 h later, CHX was added to a final concentration of 40 μg/ml, and whole-cell lysates were prepared at different time points and probed with mouse anti-V5 (*C*) or rabbit anti-mNrf2 (*D*). The graphs depict the natural logarithm of the relative expression of the V5-tagged proteins (*C*) or Gal4(HA)mNeh6 as a function of CHX-chase time (mean of two independent experiments) (*D*). The best fit lines and the derived half-lives are presented.

are conserved (amino acids 329–339 and 363–379), constructs expressing mNrf2$^{\Delta DIDLID,\Delta 329-339}$-V5, mNrf2$^{\Delta DIDLID,\Delta 363-379}$-V5 and mNrf2$^{\Delta DIDLID,\Delta 329-379}$-V5 were generated.

Initially, we compared the fractions of mNrf2$^{\Delta DIDLID}$-V5, mNrf2$^{\Delta DIDLID,\Delta 116-131}$-V5, mNrf2$^{\Delta DIDLID,\Delta 177-193}$-V5, and mNrf2$^{\Delta DIDLID,\Delta 329-339}$-V5 remaining after a 3-h CHX chase (Fig. 7*B*). Deletion of the Neh4 or the Neh5 domains from mNrf2$^{\Delta DIDLID}$-V5 protein had no obvious effect on the stability of the protein in COS1 cells. In contrast, mNrf2$^{\Delta DIDLID,\Delta 329-339}$-V5 appeared more stable than mNrf2$^{\Delta DIDLID}$-V5, although it was still subject to degradation (Fig. 7*B*). A half-life for mNrf2$^{\Delta DIDLID,\Delta 329-339}$-V5 of 2 h was calculated compared with a half-life for mNrf2$^{\Delta DIDLID}$-V5 of 40 min (Fig. 7*C*). We initially suspected that the residual instability might stem from the remaining regions of the Neh6 domain. However, whereas mNrf2$^{\Delta DIDLID,\Delta 363-379}$-V5 and mNrf2$^{\Delta DIDLID,\Delta 329-379}$-V5 were more stable than mNrf2$^{\Delta DIDLID}$-V5, they were both of equal but not greater stability than mNrf2$^{\Delta DIDLID,\Delta 329-339}$-V5 (data not shown). These results suggested that the Neh6 domain constitutes a degron and that deletion of either amino acids 329–339 or amino acids 363–379 was sufficient to inactivate completely this degron. To formally demonstrate this, we generated a construct expressing a Gal4(HA)mNeh6 fusion protein. The fusion protein was immunoreactive with rabbit anti-Gal4 serum, mouse anti-HA, and rabbit anti-mNrf2 serum (data not shown). Its half-life was considerably shorter than Gal4(HA), being ~45 min (Fig. 7*D*). Taken in total, these findings demonstrate that in stressed COS1 cells, the Neh6 domain on its own is sufficient to account for the degradation rate of the transcription factor. The instability evident when the Neh6 degron is inactivated would appear to be physiologically relevant. We infer this from the fact that inactivation of the Neh6 degron does not compromise the functionality of mNrf2$^{\Delta DIDLID}$-V5 in a transactivation assay (supplemental Fig. 3) A trivial explanation invoking misfolding of the deletion proteins, for example, would therefore appear to be insufficient to explain the residual turnover of the transcription factor. This turnover is mediated by the proteasome (data not shown), but the region(s) of Nrf2 involved in the process have yet to be unidentified.

Finally, we demonstrated that the Neh6 degron is not only sufficient but is essential for efficient turnover of Nrf2 in oxidatively stressed COS1 cells. We generated a construct expressing mNrf2-V5 lacking amino acids 329–339

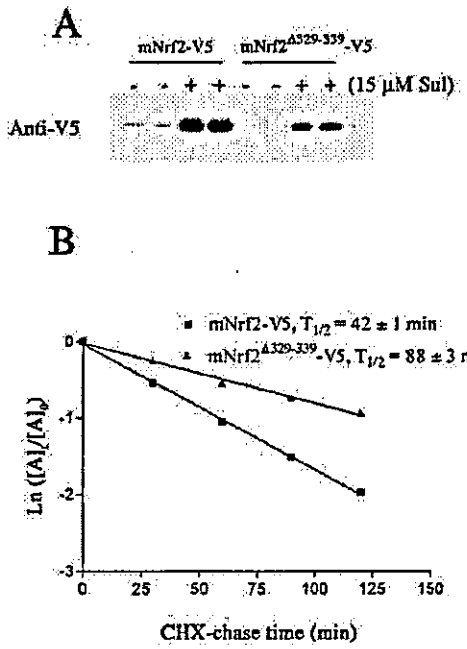

FIG. 8. **The Neh6 domain is essential for maximal turnover of Nrf2 in stressed cells.** COS1 cells in 60-mm dishes were transfected with 2 μg of a vector expressing either mNrf2-V5 or mNrf2$^{\Delta 329-339}$-V5, 2 μg of pcDNA3.1/mKeap1, and 0.8 μg of pCMVβ-gal. *A*, 24 h later, cells in duplicate dishes were treated with either 15 μM Sul (+) or vehicle (−) for 2 h, as indicated. *B*, 24 h later, CHX was added to a final concentration of 40 μg/ml, and whole-cell lysates were prepared at different time points and probed with mouse anti-V5. The graph depicts the natural logarithm of the relative expression of V5-tagged protein as a function of CHX-chase time (mean of two independent experiments). The best fit lines and derived half-lives are shown.

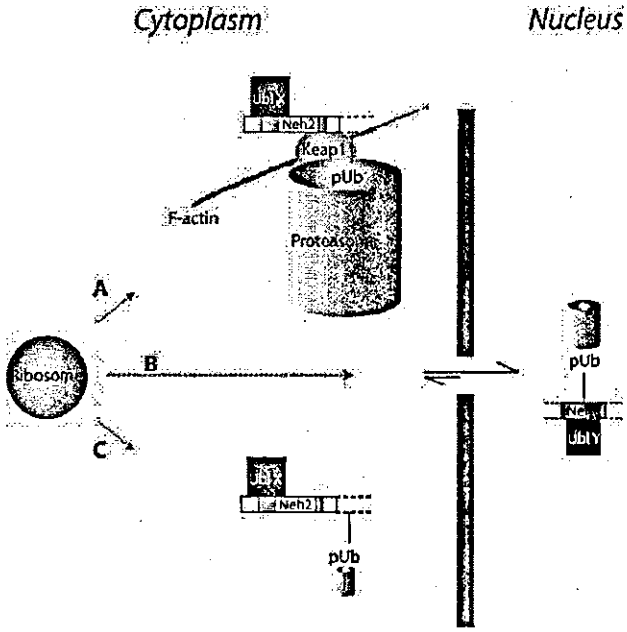

FIG. 9. **Degradation of Nrf2.** This schematic depicts the flux of Nrf2 throughout the cell. It is continuously synthesized in the cytosol by ribosomes at the ER, from where it is distributed, probably by both active and passive processes, to different regions of the cell. Continuously synthesized, it is also continuously degraded by mechanisms that vary with subcellular location. We hypothesize that at least three different spatially restricted pathways of degradation of Nrf2 may occur in cells. *A*, Keap1-dependent, DIDLID-directed degradation of Nrf2 occurs at the actin cytoskeleton. This is the most efficient mechanism for removing Nrf2, but only occurs in homeostatic cells as oxidative stress antagonizes the Nrf2-Keap1 interaction. *B*, Keap1-independent, DIDLID-directed degradation of Nrf2 occurs in the cytosol away from the actin cytoskeleton. *C*, Keap1-independent, Neh6-mediated degradation of Nrf2 occurs in the nucleus. Although less efficient than *A*, this is the predominant mode of degradation in oxidatively stressed cells. See text for further details. *Ubl X*, ubiquitin ligase recruited by the DIDLID element (shown in *green*); *Ubl Y*, ubiquitin ligase recruited by the Neh6 domain; *pUb*, polyubiquitin chain. The ETGE motif is shown in *pink*.

(mNrf2$^{\Delta 329-339}$-V5). When coexpressed with mKeap1, this protein was not impaired in its redox sensitivity. As with mNrf2-V5, it was expressed at very low levels in homeostatic cells, and its expression level was enhanced by treatment with Sul (Fig. 8*A*). However, when its half-life and the half-life of mNrf2-V5 were compared in COS1 cells after a 2-h exposure to Sul, its half-life was ~90 min, compared with 42 min for the wild-type protein (Fig. 8*B*). Thus, while the presence of Neh2 can mediate some turnover of Nrf2 in oxidatively stressed COS1 cells, the Neh6 domain is essential for its efficient turnover.

DISCUSSION

In the present paper we demonstrate for the first time that the DIDLID element within Neh2 is essential for Keap1-dependent destabilization of Nrf2. Thus, both the DIDLID element and the ETGE motif, two separate subdomains within Neh2, are required for the rapid turn over of Nrf2 under normal homeostatic conditions. Furthermore, we report also for the first time that the Neh6 domain makes the major contribution to the turn over of the transcription factor under conditions of oxidative stress. Hence, it is now proposed that at least two domains in Nrf2, the redox-sensitive Neh2 and redox-insensitive Neh6 degrons, contribute to its degradation. Based on the experimental findings reported here and those elsewhere, a model involving both these degrons that accounts for the redox-regulated turn-over of Nrf2 protein is depicted in Fig. 9. The model is justified and outlined below.

Role of the DIDLID Element—Evidence from three different cell lines indicates that the DIDLID element is critical for the destabilizing activity of the Neh2 degron. Figs. 2 and 4 demonstrate that removal of this element enhances the stability of the Gal4(HA)mNeh2 fusion protein in both the COS1- and ts20TG^{R}-transformed cell lines. Most important, this phenomenon is not restricted to transformed cell lines as it is also observed in the nontransformed rat liver RL34 epithelial cell line (supplemental Fig. 4). We propose that this element destabilizes the fusion protein by recruiting a currently unidentified ubiquitin ligase to it. The supporting evidence for this mechanistic interpretation is compelling. First, the necessity to recruit a ubiquitin ligase activity to the fusion protein is indicated by the observation that its degradation is reliant upon an intact functional ubiquitin-conjugating system (Fig. 4). Second, the notion that amino acids 17–32 recruit such an activity is suggested by the observation that deletion of this element results in a reduction in the fraction of the fusion protein that is ubiquitinated at steady state (Fig. 3). This reduction cannot be explained as a consequence of removal of a ubiquitin attachment site, as this region does not contain a lysine residue. Also, alterations in the subcellular distribution of the fusion protein, consequent upon removal of the DIDLID element, cannot be invoked to explain the reduction as immunocytochemical studies indicate that no observable differences exist between the subcellular distribution of Gal4(HA)mNeh2 and Gal4(HA)mNeh2$^{\Delta 17-32}$. Both are predominantly nuclear proteins but with a minor albeit significant fraction evident in the cytosol (data not shown). Thus, the only reasonable explanation for these findings is that the DIDLID element recruits a ubiquitin ligase activity. Formal proof, however, awaits the purifi-

cation and identification of the DIDLID-binding ubiquitin ligase activity. We propose that this ability to recruit a ligase activity underlies Neh2-mediated, Keap1-independent proteasomal degradation, and like this mode of degradation (15), it may occur constitutively and independently of the redox state of the cell.

Functional Significance of the Interaction between Neh2 and Keap1—We have demonstrated previously that the redox-sensitive protein turnover mediated by the Neh2 degron is a consequence of its direct, redox-sensitive interaction with the actin-bound (32)[3] protein Keap1. This interaction requires the presence of the ETGE tetrapeptide motif of the Neh2 domain and is abrogated by its deletion (15). The consequence of this interaction with Keap1 is that, in homeostatic cells and only homeostatic cells, the rate of degradation of both Nrf2 and Gal4(HA)mNeh2 is enhanced. Here we report for the first time that whereas the Nrf2-Keap1 interaction is necessary, it is not sufficient to increase the turnover rate of Neh2-mediated degradation. Removal of the DIDLID element maintains the interaction between the two proteins, but it does not result in an enhanced rate of degradation of Nrf2 (Figs. 5 and 6). We believe this is a consequence of the fact that Keap1 operates upon the DIDLID-directed degradation pathway and can only function in conjunction with the ubiquitin ligase activity.

In theory, Keap1 could influence the rate of Neh2-mediated degradation by enhancing the rate of ubiquitination, mediated by the DIDLID element, of the protein. This possibility seems unlikely as our previous experiments have indicated that the ubiquitination status of full-length, tagged mNrf2 in COS1 cells is not influenced by either the presence or absence of heterologous mKeap1, the deletion of the ETGE tetrapeptide, or treatment with Sul all under conditions where mKeap1 does influence its half-life (15). Alternatively, as pointed out by Pickart (33), the *in vivo* concentration of ubiquitinated protein can be sufficiently high that transfer of ubiquitinated substrates to the proteasome may be rate-limiting, and therefore altering the rate of transfer of a specific ubiquitinated substrate to the proteasome, relative to generic substrates, is another way of controlling its turnover rate. Although it is conceivable that recruitment by Keap1 of Nrf2 to the cytoskeleton suffices to enhance the transfer of the transcription factor to the proteasome, a biologically more interesting possibility is that Keap1 actually associates with the proteasome. Indeed, a large body of experimental evidence demonstrates that numerous proteins bind to the proteasome in order to modulate the rate at which specific substrates are transferred to it (reviewed in Ref. 34). These include proteins such as Ubl/Uba (ubiquitin-associated)-containing proteins, and ubiquitin ligases (34–36). Of greater relevance to this discussion is a group of miscellaneous proteins with no obvious connection to the ubiquitination system but that affect the degradation of specific proteins by interacting with the proteasome. The yeast protein Cic1 was originally identified in a yeast two-hybrid screen for proteins interacting with the α4 subunit of the yeast proteasome (37). It has no effect on the global rate of proteasomal degradation, but in its absence the rates of degradation of two specific substrates (the SCF subunits Cdc4 and Grr1) are retarded. However, it does not influence their ubiquitination status. Instead, it has been proposed to act as an adaptor between the relevant SCF complexes and the proteasome, thereby ensuring the preferential degradation of important regulatory proteins over the general population of ubiquitinated substrates (37). Gankyrin and Homer3A11 bind the S6 and S8 ATPase subunits, respectively, of the base of the 19 S regulator of the 26 S proteasome. As with Cic1, they have been postulated to enhance the rate of degradation of their interacting partners, such as retinoblastoma protein and metabotropic glutamate receptors, by enhancing substrate targeting to the proteasome (38–40).

By analogy with the above examples, we propose that Keap1 increases the rate of transfer of ubiquitinated Nrf2 to the proteasome above the rate observed for the general population of ubiquitinated substrates by associating with the proteasome. It should be noted that there is a precedent for binding of Kelch-repeat proteins to the proteasome. Vidal and co-workers (41) screened a *C. elegans* cDNA library by yeast two-hybrid analysis by using 30 26 S proteasome subunits as bait. One cDNA isolated, W02G9.2, encodes a member of the Kelch-repeat family and was found to interact with the α 2, 4, 5, and 6 proteasome subunits in independent screens. Like Keap1, this protein contains an N-terminal BTB domain and 6 Kelch motifs. These proteins are 28% identical and 44% similar. Of the 16 Kelch-repeat proteins encoded by the *C. elegans* genome (42), W02G9.2 is the second-most similar to Keap1. This sequence similarity suggests that both proteins may mediate similar protein-protein interactions.

Keap1 may destabilize Nrf2 by mechanisms other than that evident in COS1 cells. Although we find no evidence that Keap1 influences the ubiquitination status of Nrf2 under conditions where it destabilizes it, the work of Zhang and Hannink (43) strongly suggests that Keap1 may indeed do so, at least in certain cellular contexts. They have proposed that Keap1 acts as a ubiquitin ligase (43). This is in agreement with the recent observation by others that BTB domains recruit Cul3-based ubiquitin ligase activities (44–47). Thus, Keap1 may recruit Cul3 via its BTB domain and Nrf2 via one of its Kelch repeats. The differences between our results and those presented by Zhang and Hannink (43) presumably reflect differences in the proteome expressed, or its subcellular disposition, in our respective model systems. It will be of interest to determine whether Keap1 can function both to enhance the rate of degradation mediated by the DIDLID element and itself recruit a ubiquitin ligase under physiological conditions or whether one or the other predominates in different organ/cell types.

The Neh6 Degron—Inactivation of the Neh2 degron by deletion of the DIDLID element only modestly stabilized Nrf2. Indeed, under conditions of oxidative stress the absence of Neh2-mediated degradation was largely irrelevant from the point of view of turn over of Nrf2. We hypothesized that there must be another degron that controlled the rate of degradation of Nrf2 in stressed cells. The Neh6 domain was shown to be such a degron (Fig. 7). It should be noted that other regions also contribute to proteasomal degradation of Nrf2 as inactivation of both the Neh2 degron and the Neh6 degron still left a protein with a half-life of 2 h. Although little is known about Neh6 at present, our data support the following two observations. First, Keap1 is incapable of enhancing the rate of degradation mediated by this degron. Thus mKeap1 can interact with $mNrf2^{\Delta 17-32}$-V5, but cannot influence its half-life in homeostatic cells (Fig. 6). Second, the presence of the Neh6 degron is essential for maximal turnover of the transcription factor in oxidatively stressed COS1 cells (Fig. 8). This is despite the fact that, at least in the context of Gal4(HA) fusion proteins, there is not any great difference in the efficiency of degradation mediated by the DIDLID element or the Neh6 domain (*cf.* Fig. 2 with Fig. 7).

Degradation of the Nrf2 Transcription Factor—We now present the broad outlines of a model accounting for the degradation of the Nrf2 transcription factor (Fig. 9). This model accommodates the following facts: Keap1 does not influence the rate of degradation directed by the Neh6 degron, the DIDLID ele-

[3] M. McMahon and J. D. Hayes, unpublished data.

ment does not make a major contribution to the degradation of Nrf2 in oxidatively stressed cells, and finally that the degradation of Nrf2 in homeostatic cells does not follow first-order kinetics. The salient features of this model are as follows.

(i) Keap1 contains reactive cysteine residues, and in oxidatively stressed cells these are modified leading to a conformational change that prevents its interaction with Nrf2 (48). Under such conditions, Keap1 cannot bind to and enhance the transfer of ubiquitinated Nrf2 (directed by the DIDLID element) to the proteasome. Nor can the modified Keap1 passively bind to nonubiquitinated Nrf2. In fact, in stressed cells Nrf2 is exclusively nuclear (15). Such a location reduces the opportunity for DIDLID-directed ubiquitination of Nrf2 (see point ii, below). As a result, in stressed cells Nrf2 is subjected primarily to Neh6-mediated degradation. We hypothesize that the Neh6 degron is functional only in the nucleus probably due to the fact that the proteins required for this function (presumably a ubiquitin ligase activity) are restricted to this compartment. As Keap1 is restricted to the cytoplasm, this provides a simple explanation for the observation that Keap1 cannot enhance degradation mediated by the Neh6 domain.

(ii) In homeostatic cells, Keap1 enhances the rate of DIDLID-directed degradation of Nrf2 by enhancing the rate of transfer of its polyubiquitinated form to a subset of proteasomes defined by the presence of an associated Keap1 protein(s). In some cell types, Keap1 may also enhance the rate of ubiquitination of Nrf2 in homeostatic cells via an associated ubiquitin ligase activity, most likely a Cul3-based ligase, recruited via the BTB domain. As Keap1 is restricted to the actin cytoskeleton, we infer that the putative ubiquitin ligase recruited by the DIDLID element must have access to this region of the cell. Although it is not necessary that the ubiquitin ligase is exclusively associated with the cytoskeleton, we suggest that it is excluded from the nucleus. Given that Nrf2 is predominantly nuclear in stressed cells, this would explain why the DIDLID element plays no major role in the turnover of Nrf2 in stressed cells.

(iii) As Keap1 is spatially restricted to the actin cytoskeleton, Keap1-dependent degradation must also be so restricted. On the basis of data in this paper, we postulate that both Keap1-dependent and Keap1-independent degradation occur simultaneously in different regions of homeostatic cells. The results presented in Fig. 6*B* suggests that degradation of mNrf2-V5 in homeostatic cells follows biphasic kinetics. The second phase of degradation is slower than the first and is indistinguishable from Keap1-independent degradation kinetics. We do not believe that this is coincidental. We propose that the biphasic degradation results from the superimposition of simultaneously operative Keap1-dependent and Keap1-independent degradation pathways in homeostatic cells, both pathways following first-order kinetics. The initial rapid degradation of Nrf2 after addition of CHX results from the predominance, initially, of Keap1-dependent degradation of Nrf2 in the vicinity of Keap1; during later times, as the concentration of Nrf2 in this region of the cell is reduced, Keap1-independent degradation of Nrf2 out with the environs of Keap1 predominates.[4] Unfortunately, the low level of mNrf2-V5 in homeostatic COS1 cells has so far precluded an empirical determination of its distribution.

(iv) Finally, the ultrastructure of the cell may have one final consequence for Keap1-dependent degradation of Nrf2 in homeostatic cells. As there is a constant flux of Nrf2 through the cell (it is constantly created and destroyed), kinetic factors become as important as thermodynamic factors in determining its ultimate fate. We are therefore intrigued by the observation of Diehl and co-workers (49) that Keap1 appears to colocalize with calreticulin, an endoplasmic reticulum (ER)-resident protein. Such a notion is not necessarily in conflict with the idea that Keap1 is actin-bound, as there is data in the literature suggesting an association between the architecture of the ER and the actin cytoskeleton (50–52). Protein synthesis does not occur uniformly throughout the cell but occurs primarily at the ER. The possibility exists that at least a portion of Keap1 might be coincident with the site of Nrf2 synthesis. Such a pool of Keap1 might be kinetically favored to interact with newly translated Nrf2. This may be important to ensure that Keap1-dependent degradation, the most efficient pathway of Nrf2 degradation, is predominant in homeostatic cells.

Although this model is speculative, particularly with regard to the influence of cell ultrastructure upon the rate of degradation of Nrf2, we believe it is both valid and useful. It is valid because it is sufficiently powerful to explain many of the features of Keap1-dependent regulation of Nrf2 that have been reported by us and other workers in the field, and it is useful because it provides a framework for the design of further experiments that in turn will cast light on the validity or otherwise of its basic tenets.

Concluding Comments—In this paper we have ascribed a function to the previously uncharacterized Neh6 domain. This domain appears to be specific to Nrf2 as BLAST searches have failed to identify its conserved primary sequences in other proteins. Of greater general interest perhaps, we have demonstrated that the DIDLID element is essential for the ubiquitination of Nrf2 and its rapid turn over during homeostatic conditions. This element can also be found in the related protein Nrf1, which also contains the ETGE motif, suggesting that at least some of the splice variants of this transcription factor are regulated in a similar fashion to Nrf2. Both Nrf1 and Nrf2 appear to be responsible for cellular adaptation to oxidative stress in vertebrates from human to fish (19, 53). In the more distantly related *C. elegans*, which belongs to a different metazoan clade from that of the vertebrates, adaptation to such stress relies upon the SKN-1 protein, which also contains a DIDLID element (54). Although we are unaware of any data pertaining to SKN-1 protein stability, this raises the intriguing possibility that redox-regulated transcription factor turn over is a mechanism of adaptation to oxidative stress that evolved early in the evolution of the metazoan lineage.

Acknowledgments—We are indebted to Profs. H. Ozer (University of Medicine and Dentistry of New Jersey) and C. Borner (University of Freiburg, Germany) for their gift of the ts20TG^R and H38.5 cells.

REFERENCES

1. Itoh, K., Chiba, T., Takahashi, S., Ishii, T., Igarashi, K., Katoh, Y., Oyake, T., Hayashi, N., Satoh, K., Hayatama, I., Yamamoto, M., and Nabeshima, Y.-I. (1997) *Biochem. Biophys. Res. Commun.* 236, 313–322
2. McMahon, M., Itoh, K., Yamamoto, M., Chanas, S. A., Henderson, C. J., McLellan, L. I., Wolf, C. R., Cavin, C., and Hayes, J. D. (2001) *Cancer Res.* 61, 3299–3307
3. Kwak, M.-K., Wakabayashi, N., Itoh, K., Motohashi, H., Yamamoto, M., and

[4] We do not doubt the observation that both Keap1-dependent and -independent pathways of degradation occur simultaneously in our population of homeostatic COS1 cells nor the hypothesis that, given the ordered structure of the cell, both processes will occur simultaneously within the one cell. Nonetheless, it must be noted that our experimental strategy cannot distinguish between both pathways occurring intracellularly or, alternatively, occurring intercellularly. In particular, the transient transfection procedure will give rise to a heterogeneous population of cells possessing varying ratios of mKeap1 and mNrf2-expressing plasmids approximately in accordance with the binomial distribution. It is therefore possible that in some cells mNrf2-V5 cannot be degraded by a Keap1-dependent process. Also, it is unlikely that all cells in the population have the same redox potential as this characteristic varies with cell state. Therefore, some cells in the population are likely to experience oxidative stress even in the absence of Sul treatment.

Kensler, T. W. (2003) *J. Biol. Chem.* **278**, 8135–8145
4. Chan, K., and Kan, Y. W. (1999) *Proc. Natl. Acad. Sci. U. S. A.* **96**, 12731–12736
5. Aoki, Y., Sato, H., Nishimura, N., Takahashi, S., Itoh, K., and Yamamoto, M. (2001) *Toxicol. Appl. Pharmacol.* **173**, 154–160
6. Cho, H.-Y., Jedlicka, A. E., Reddy, S. P. M., Kensler, T. W., Yamamoto, M., Zhang, L.-Y., and Kleeberger, S. R. (2002) *Am. J. Respir. Cell Mol. Biol.* **26**, 175–182
7. Lee, J.-M., Shih, A. Y., Murphy, T. H., and Johnson, J. A. (2003) *J. Biol. Chem.* **278**, 37948–37956
8. Nguyen, T., Sherratt, P. J., and Pickett, C. B. (2003) *Annu. Rev. Pharmacol. Toxicol.* **43**, 233–260
9. Motohashi, H., O'Connor, T., Katsuoka, F., Engel, J. D., and Yamamoto, M. (2002) *Gene (Amst.)* **294**, 1–12
10. Motohashi, H., Katsuoka, F., Shavit, J. A., Engel, J. D., and Yamamoto, M. (2000) *Cell* **103**, 865–875, and references therein
11. Sun, Y., Hoshino, H., Takaku, K., Nakajima, O., Muto, A., Suzuki, H., Tashiro, S., Shibahara, S., Alam, J., Taketo, M. M., Yamamoto, M., and Igarashi, K. (2002) *EMBO J.* **21**, 5216–5224
12. Venugopal, R., and Jaiswal, A. K. (1996) *Proc. Natl. Acad. Sci. U. S. A.* **93**, 14960–14965
13. Kwak, M.-K., Itoh, K., Yamamoto, M., and Kensler, T. W. (2002) *Mol. Cell. Biol.* **22**, 2883–2892
14. Itoh, K., Wakabayashi, N., Katoh, Y., Ishii, T., O'Connor, T., and Yamamoto, M. (2003) *Genes Cells* **8**, 379–391
15. McMahon, M., Itoh, K., Yamamoto, M., and Hayes, J. D. (2003) *J. Biol. Chem.* **278**, 21592–21600
16. Suzuki, H., Tashiro, S., Sun, J., Satomi, S., and Igarashi, K. (2003) *J. Biol. Chem.* **278**, 49246–49253
17. Nioi, P., McMahon, M., Itoh, K., Yamamoto, M., and Hayes, J. D. (2003) *Biochem. J.* **374**, 337–348
18. Itoh, K., Wakabayashi, N., Katoh, Y., Ishii, T., Igarashi, K., Engel, J. D., and Yamamoto, M. (1999) *Genes Dev.* **13**, 76–86
19. Kobayashi, M., Itoh, K., Suzuki, T., Osanai, H., Nishikawa, K., Katoh, Y., Takagi, Y., and Yamamoto, M. (2002) *Genes Cells* **7**, 807–820
20. Stewart, D., Killeen, E., Naquin, R., Alam, S., and Alam, J. (2003) *J. Biol. Chem.* **278**, 2396–2402
21. Nguyen, T., Sherratt, P. J., Huang, H.-C., Yang, C. S., and Pickett, C. B. (2003) *J. Biol. Chem.* **278**, 4536–4541
22. Walker, A. K., See, R., Batchelder, C., Kophengnavong, T., Gronniger, J. T., Shi, Y., and Blackwell, T. K. (2000) *J. Biol. Chem.* **275**, 22166–22171
23. Salghetti, S. E., Muratani, M., Wijnen, H., Futcher, B., and Tansey, W. P. (2000) *Proc. Natl. Acad. Sci. U. S. A.* **97**, 3118–3123, and references therein
24. Favreau, L. V., and Pickett, C. B. (1991) *J. Biol. Chem.* **266**, 4556–4561
25. Treier, M., Staszewski, L., and Bohmann, D. (1994) *Cell* **78**, 787–796
26. Chowdary, D. R., Dermody, J. J., Jha, K. K., and Ozer, H. L. (1994) *Mol. Cell. Biol.* **14**, 1997–2003
27. Verma, R., and Deshaies, R. J. (2000) *Cell* **101**, 341–344
28. Asher, G., Lotem, J., Sachs, L., Kahana, C., and Shaul, Y. (2002) *Proc. Natl. Acad. Sci. U. S. A.* **99**, 13125–13130
29. Kalejta, R. F., and Shenk, T. (2003) *Proc. Natl. Acad. Sci. U. S. A.* **100**, 3263–3268
30. Sheaff, R. J., Singer, J. D., Swanger, J., Smitherman, M., Roberts, J. M., and Clurman, B. E. (2000) *Mol. Cell* **5**, 403–410
31. Katoh, Y., Itoh, K., Yoshida, E., Miyagashi, M., Fukamizu, A., and Yamamoto, M. (2001) *Genes Cells* **6**, 857–868
32. Kang, M.-I., Kobayashi, A., Wakabayashi, N., Kim, S.-G., and Yamamoto, M. (2004) *Proc. Natl. Acad. Sci. U. S. A.* **101**, 2046–2051
33. Pickart, C. M. (2000) *Trends Biochem. Sci.* **25**, 544–548
34. Hartmann-Petersen, R., Seeger, M., and Gordon, C. (2003) *Trends Biochem. Sci.* **28**, 26–31
35. Glockzin, S., Ogi, F.-X., Hengstermann, A., Scheffner, M., and Blattner, C. (2003) *Mol. Cell. Biol.* **23**, 8960–8969
36. Xie, Y., and Varshavsky, A. (2002) *Nat. Cell Biol.* **4**, 1003–1007
37. Jäger, S., Strayle, J., Heinemeyer, W., and Wolf, D. H. (2001) *EMBO J.* **20**, 4423–4431
38. Dawson, S., Apcher, S., Mee, M., Higashitsuji, H., Baker, R., Uhle, S., Dubiel, W., Fujita, J., and Mayer, R. J. (2002) *J. Biol. Chem.* **277**, 10893–10902
39. Rezvani, K., Mee, M., McIlhinney, J., and Mayer, R. J. (2003) *Biochem. Soc. Trans.* **31**, 470–473
40. Krzywda, S., Brzozowski, A. M., Higashitsuji, H., Fujita, J., Welchman, R., Dawson, S., Mayer, R. J., and Wilkinson, A. J. (2004) *J. Biol. Chem.* **279**, 1541–1545
41. Davy, A., Bello, P., Thierry-Mieg, N., Vaglio, P., Hitti, J., Doucette-Stamm, L., Thierry-Mieg, D., Reboul, J., Boulton, S., Walhout, A. J. M., Coux, O., and Vidal, M. (2001) *EMBO Rep.* **2**, 821–828
42. Prag, S., and Adams, J. C. (2003) *BMC Bioinformatics* http://www.biomedcentral.com/1471-2105/4/42
43. Zhang, D. D., and Hannink, M. (2003) *Mol. Cell. Biol.* **23**, 8137–8151
44. Pintard, L., Willis, J. H., Willems, A., Johnson, J.-L. P., Srayko, M., Kurz, T., Glaser, S., Mains, P. E., Tyers, M., Bowerman, B., and Peter, M. (2003) *Nature* **425**, 311–316
45. Xu, L., Wei, Y., Reboul, J., Vaglio, P., Shin, T.-H., Vidal, M., Elledge, S. J., and Harper, J. W. (2003) *Nature* **425**, 316–321
46. Geyer, R., Wee, S., Anderson, S., Yates, J., III, and Wolf, D. A. (2003) *Mol. Cell* **12**, 783–790
47. Furukawa, M., He, Y. J., Borchers, C., and Xiong, Y. (2003) *Nat. Cell Biol.* **5**, 1001–1007
48. Wakabayashi, N., Dinkova-Kostova, A. T., Holtzclaw, W. D., Kang, M.-I., Kobayashi, A., Yamamoto, M., Kensler, T. W., and Talalay, P. (2004) *Proc. Natl. Acad. Sci. U. S. A.* **101**, 2040–2045
49. Cullinan, S. B., Zhang, D., Hannink, M., Arvisais, E., Kaufman, R. J., and Diehl, J. A. (2003) *Mol. Cell. Biol.* **23**, 7198–7209
50. Boevink, P., Oparka, K., Santa Cruz, S., Martin, B., Betteridge, A., and Hawes, C. (1998) *Plant J.* **15**, 441–447, and references therein
51. Wöllert, T., Weiss, D. G., Gerdes, H.-H., and Kuznetsov, S. A. (2002) *J. Cell Biol.* **159**, 571–577, and references therein
52. Shimada, O., Hara-Kuge, S., Yamashita, K., Tosaka-Shimada, H., Yanchao, L., Yongnan, L., Atsuni, S., and Ishikawa, H. (2003) *Cell Struct. Funct.* **28**, 155–163, and references therein
53. Leung, L., Kwong, M., Hou, S., Lee, C., and Chan, J. Y. (2003) *J. Biol. Chem.* **278**, 48021–48029
54. An, J. H., and Blackwell, T. K. (2003) *EMBO J.* **17**, 1882–1893

The FASEB Journal • FJ Express

The transcription factor NRF2 protects against pulmonary fibrosis

HYE-YOUN CHO,*,†,[1] SEKHAR P. M. REDDY,* MASAYUKI YAMAMOTO,‡ AND STEVEN R. KLEEBERGER*,†

*Department of Environmental Health Sciences, The Johns Hopkins University Bloomberg School of Public Health, Baltimore, Maryland, USA; †Laboratory of Respiratory Biology, National Institute of Environmental Health Sciences, National Institutes of Health, Research Triangle Park, North Carolina, USA; and ‡Institute of Basic Medical Sciences and Center for Tsukuba Advanced Research Alliance, University of Tsukuba, Tennoudai, Tsukuba, Japan

To read the full text of this article, go to http://www.fasebj.org/cgi/doi/10.1096/fj.03-1127fje; doi: 10.1096/fj.03-1127fje

SPECIFIC AIMS

Molecular mechanisms of fibrosis are poorly understood, although reactive oxygen species (ROS) are thought to have an important role. The primary objective of this study was to determine whether NF-E2-related factor 2 (NRF2), a key transcriptional regulator for antioxidant response element (ARE) -mediated induction of cellular antioxidants and detoxifying proteins, protects against pathogenesis of pulmonary fibrosis. To test this hypothesis, we exposed mice with targeted deletion of *Nrf2* (ICR/Sv129-*Nrf2*$^{-/-}$) and wild-type (ICR/Sv129-*Nrf2*$^{+/+}$) mice to bleomycin and compared pulmonary injury and fibrotic responses.

PRINCIPAL FINDINGS

1. Effects of targeted disruption of *Nrf2* on lung injury and fibrosis phenotypes

Mice (male, 6–10 wk) were anesthetized with 1.39 mg ketamine and 0.22 mg xylozine in saline (0.1 mL, i.p.), and a single dose (1.5 or 3.2 U/kg) of bleomycin in saline (1.25 U/mL) was delivered by intratracheal instillation. An equivalent volume of saline was instilled in control mice of each genotype. A significantly greater increase (40%) in lung/body weight ratio (a parameter of lung edema and matrix deposition) was found in *Nrf2*$^{-/-}$ mice compared with *Nrf2*$^{+/+}$ mice 6 days after bleomycin (3.2 U/kg). Bleomycin (3.2 U/kg) significantly increased (33%) lung hydroxyproline content (a marker of collagen deposition) over *Nrf2*$^{-/-}$ vehicle controls; no changes were found in *Nrf2*$^{+/+}$ mice. The lower dose of bleomycin (1.5 U/kg) was used to investigate prefibrotic molecular and cellular events as well as time-dependent changes in pathology. Fourteen days after bleomycin (1.5 U/kg) instillation, a significantly greater loss of body weight was found in *Nrf2*$^{-/-}$ mice, relative to *Nrf2*$^{+/+}$ mice. Mean numbers of total cells, neutrophils, lymphocytes, and epithelial cells recovered in bronchoalveolar lavage fluid were significantly higher (~2 to 3-fold) in *Nrf2*$^{-/-}$ mice than in *Nrf2*$^{+/+}$ mice 14 days after low dose (**Fig. 1**) and 6 days after high dose bleomycin (data not shown). Compared with *Nrf2*$^{+/+}$ mice, lung collagen accumulation determined by Sirius red dye-collagen binding assay was significantly greater in *Nrf2*$^{-/-}$ mice 3, 7, and 14 days after bleomycin treatment. Statistically significant deposition of collagen in *Nrf2*$^{+/+}$ mice was found only at 14 days after bleomycin.

2. Effects of targeted disruption of *Nrf2* on pulmonary pathology

Histological staining (Sirius red/Fast green, H&E) of lung tissue sections indicated significant differences in progression of pulmonary injury, inflammation, and fibrosis between *Nrf2*$^{-/-}$ and *Nrf2*$^{+/+}$ mice (**Fig. 2**). Predominant histopathologic features of *Nrf2*$^{-/-}$ mice instilled with bleomycin (1.5 U/kg) included alveolar inflammation (principally neutrophils and lymphocytes), diffused fibrotic patch formation with collagen accumulation, hyperplastic and hypertrophic changes of epithelium lining alveoli, small bronchi, and terminal bronchioles. Fibrogenesis was observed primarily in alveolar interstitium adjacent to terminal bronchioles, and alveolar bronchiolization was distinct in areas undergoing severe fibrotic remodeling. Compared with *Nrf2*$^{-/-}$ mice, relatively mild inflammation and only focal fibrotic lesions were found in *Nrf2*$^{+/+}$ mice at 7 days. Persistent inflammation and abnormal lung architecture characterized by extensive fibroblast proliferation, alveolar bronchiolization, and collagen-stained matrix deposition was evident in *Nrf2*$^{-/-}$ mice 14 days after

[1] Correspondence: Laboratory of Respiratory Biology, NIEHS, NIH, Research Triangle Park, North Carolina 27709, USA. E-mail: cho2@niehs.nih.gov

0892-6638/04/0018-1258 © FASEB

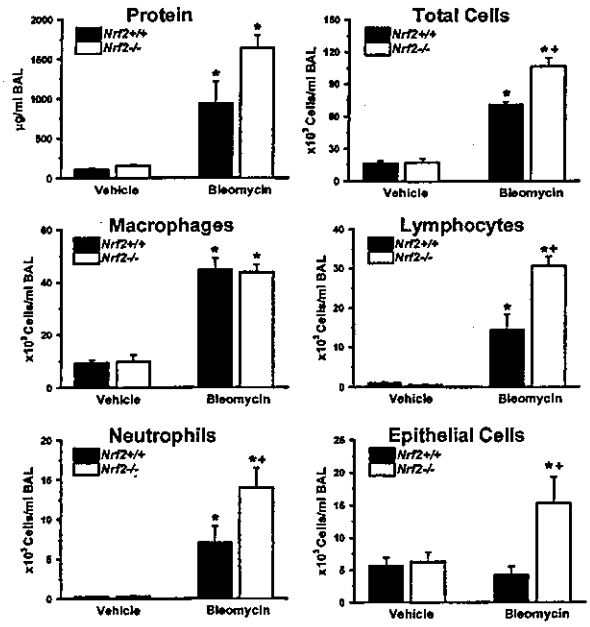

Figure 1. Effect of targeted disruption of *Nrf2* on bleomycin (1.5 U/kg)-induced increases in bronchoalveolar lavage phenotypes 14 days after instillation. Data are presented as means ± SEM (n=4–5/group). *Significantly different from genotype-matched vehicle control mice ($P<0.05$). +Significantly different from bleomycin-treated $Nrf2^{+/+}$ mice ($P<0.05$).

instillation. Fibrosis scoring by Ashcroft method ranging from 0 (no fibrosis) to 8 (total fibrosis) demonstrated that significant lung fibrosis was evident at 7 and 14 days postinstillation in both genotypes of mice. However, average fibrotic scores were significantly higher in $Nrf2^{-/-}$ mice compared with $Nrf2^{+/+}$ mice at 7 days (60%; 4.98±0.32 vs. 3.16±0.33) and 14 days (27%; 6.77±0.46 vs. 5.31±0.45) after bleomycin.

3. Bleomycin-Induced mRNA/Protein expression and transactivation of lung NRF2

Bleomycin caused significant time-dependent induction of NRF2 mRNA expression in lungs of $Nrf2^{+/+}$ mice (50% over saline controls at 14 days). Immunoblotting analyses detected marked bleomycin-induced increases of cytoplasmic and nuclear NRF2 accumulation in lungs of $Nrf2^{+/+}$ mice (14 days after instillation). Time-dependent increase of bleomycin-induced nuclear NRF2-DNA (NF-E2) binding activity was detected by gel mobility shift/supershift analysis in lungs of $Nrf2^{+/+}$ mice.

4. Effects of targeted disruption of *Nrf2* on bleomycin-induced antioxidant enzyme expression

Bleomycin caused up-regulation of mRNA for NAD-P(H):quinone oxidoreductase (NQO1), glutathione-S-transferase (GST)-Ya (α)/-Yp1 (pi)/-Yb1 (mu), catalytic (GLCLc) and regulatory (GLCLr) subunits of gamma glutamylcysteine ligase, thioredoxin reductase (TXNRD) 1, UDP glycosyl transferase 1a6, carboxylesterase (Ex), heme oxygenase (HO)-1, glutathione peroxidase (GPx) 2, and superoxide dismutase (SOD)-3 in $Nrf2^{+/+}$ mice over basal levels. Bleomycin-induced expression of all these genes was significantly higher in $Nrf2^{+/+}$ mice than in $Nrf2^{-/-}$ mice. Among these, mRNA levels of NQO1, TXNRD1, GLCLc, Ex, and GPx2 were constitutively attenuated in $Nrf2^{-/-}$ mice compared with $Nrf2^{+/+}$ mice, and their steady-state expression levels were not significantly altered by bleomycin instillation in $Nrf2^{-/-}$ mice. Consistent with gene expression results, bleomycin-induced protein levels of pulmonary GST-α, GST-mu, GPx, and HO-1 were significantly greater in $Nrf2^{+/+}$ mice than in $Nrf2^{-/-}$ mice, with peaks at 7 days. No statistically significant changes were detected in $Nrf2^{-/-}$ mice after bleomycin.

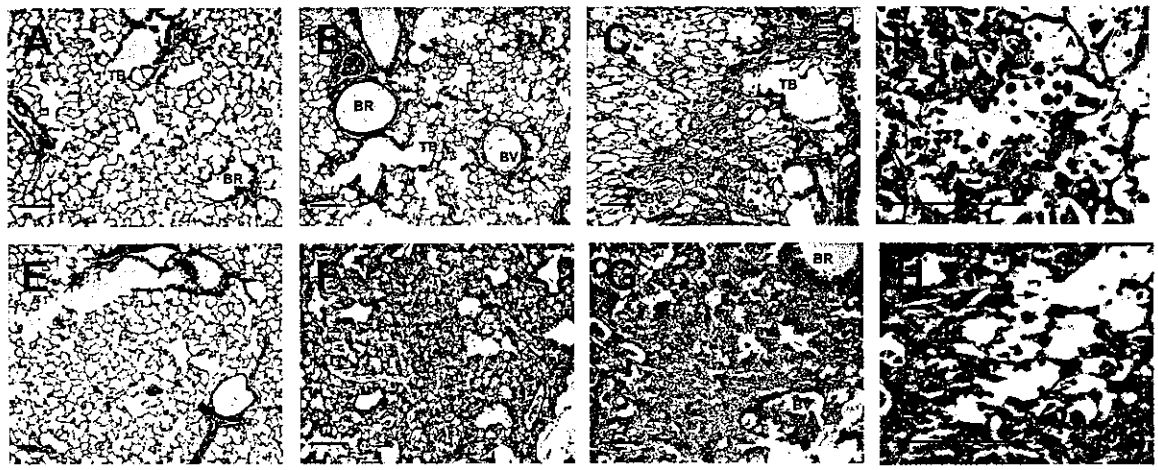

Figure 2. Differential progression of pulmonary injury and fibrosis in $Nrf2^{+/+}$ (*A–D*) and $Nrf2^{-/-}$ (*E–H*) mice after bleomycin (1.5 U/kg). Paraffin-embedded left lung tissue sections were processed for histological analyses and Sirius red/Fast green staining was performed to visualize collagen deposition (red dye staining) in control lungs (*A, E*) or fibrotic lung interstitium 7 (*B, F*) or 14 days (*C, G*) after bleomycin. Higher magnification of H&E-stained lung tissue sections illustrates alveolar bronchiolization in fibrotic lesions of $Nrf2^{+/+}$ (*D*) and $Nrf2^{-/-}$ (*H*) mice 14 days after bleomycin. Arrows, bronchiolization; TB, terminal bronchiole; BR, bronchiole; BV, blood vessel. Bar: 100 μm.

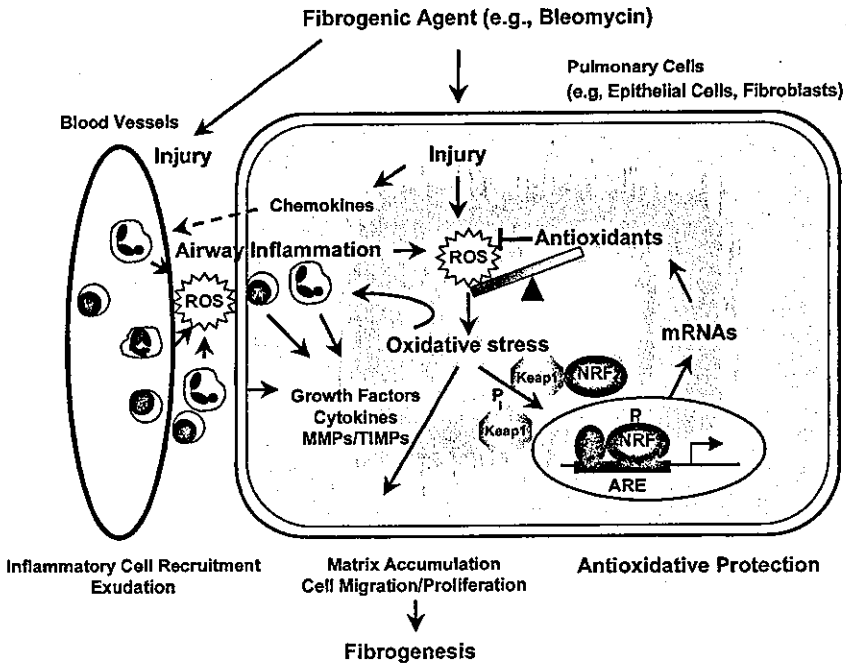

Figure 3. A hypothetical mechanism depicts a protective role of NRF2 in the pathogenesis of pulmonary fibrosis. Imbalance of cellular oxidant (ROS) and of antioxidant capacity induced by injury and inflammation causes oxidative stress in pulmonary cells. It may cause prefibrotic events (e.g., activation of growth factors) leading to matrix deposition and fibroblast proliferation. Oxidative stress may also trigger modification (e.g., phosphorylation) of Keap1-NRF2 sensor to release NRF2 from the complex. NRF2 binding to ARE in association with other transcription factor (e.g., small Maf, c-Jun) can induce transcriptional activation of antioxidant/detoxifying proteins to combat against ROS and further oxidative injury.

5. Effects of targeted disruption of *Nrf2* on bleomycin-induced lung injury/fibrosis marker expression

Greater accumulation of transcripts for several matrix markers of fibroproliferation (type 1 collagen α 2; Col1a2, fibronectin 1; FN1, tenascin-C) and pulmonary injury and remodeling markers (transforming growth factor-βs; TGF-βs, matrix metalloproteinases; MMPs, tissue inhibitor of metalloproteinase 1; TIMP1) was found in $Nrf2^{-/-}$ mice compared with $Nrf2^{+/+}$ mice after bleomycin. Transcripts of many of these genes were constitutively higher in $Nrf2^{-/-}$ mice than in $Nrf2^{+/+}$ mice, while tenascin-C and MMP7 were not detected in control lung tissues. Consistent with gene expression results, protein levels of lung MMP2, TGF-β, connective tissue growth factor (CTGF), and tenascin-C were significantly higher in $Nrf2^{-/-}$ mice than in $Nrf2^{+/+}$ mice after instillation (7 or 14 days postinstillation).

CONCLUSIONS AND SIGNIFICANCE

Results of the present study supported the hypothesis that NRF2 is protective against fibrotic lung injury. Relative to $Nrf2^{+/+}$ mice, targeted deletion of *Nrf2* significantly enhanced susceptibility to murine pulmonary inflammation and fibrosis induced by the anti-neoplastic drug bleomycin. Suppressed induction of NRF2-dependent antioxidant/defense enzymes in lungs of $Nrf2^{-/-}$ mice suggests that these enzymes may contribute to NRF2-mediated protection against bleomycin-induced lung fibrosis. This is the first study to suggest an upstream regulatory mechanism of cellular antioxidant enzyme defense in an experimental fibrosis model.

Fibrosis is an increasingly prevalent disorder, and is an end-state process in a number of chronic diseases of kidney, liver, and lung. In particular, idiopathic pulmonary fibrosis is a progressive and usually fatal disease of unknown etiology with no known effective therapy. A role for oxidants in the pathogenesis of pulmonary fibrosis has been suggested in previous studies. Protective roles of antioxidative mechanisms in pulmonary fibrosis were demonstrated by examining the role of enzymatic (e.g., SODs) or nonenzymatic (e.g., N-acetylcysteine) antioxidants. The thiol redox system (glutathione, thioredoxin) was also determined to be protective against lung fibrosis. The present study supports this concept, and provides a novel molecular mechanism through which antioxidative protection against fibrogenesis may occur. It is, however, important to note that antioxidative mechanism mediated by ARE-NRF2 response was not sufficient to completely ameliorate inflammation and fibrotic responses to bleomycin. Other antifibrotic mechanisms (e.g., interleukins-9 and 12) may interact for protection against fibrosis.

The present study demonstrated that bleomycin caused increased mRNA expression, lung protein levels, and nuclear DNA binding of NRF2 in advance of the onset of pulmonary inflammation and fibrogenesis. As depicted in **Fig. 3**, our findings suggest that activation of NRF2 and ARE-mediated induction of antioxidant defense enzymes during pathogenesis of ROS-mediated fibrogenesis has a key role in combating ROS and suppression of fibrotic tissue injury. Results from the current study may have important implications for development of combined therapies for bleomycin-toxicity and idiopathic pulmonary fibrosis to complement anti-inflammation therapy, which is only effective in subsets of fibrosis patients. FJ

Available online at www.sciencedirect.com
SCIENCE DIRECT®
Biochemical and Biophysical Research Communications 320 (2004) 62–69
BBRC
www.elsevier.com/locate/ybbrc

MafT, a new member of the small Maf protein family in zebrafish☆

Yaeko Takagi, Makoto Kobayashi,* Li Li, Takafumi Suzuki, Keizo Nishikawa, and Masayuki Yamamoto

ERATO-JST, Center for TARA and Institute of Basic Medical Sciences, University of Tsukuba, 1-1-1 Tennodai, Tsukuba 305-8575, Japan

Received 2 April 2004
Available online 7 June 2004

Abstract

Small Maf proteins play critical roles on morphogenesis and homeostasis through associating with CNC proteins. To date, three small Maf proteins, MafF, MafG, and MafK, have been reported in vertebrates, which share redundant functions. In this study, we tried to identify and characterize small Maf proteins in zebrafish to elucidate their conservation and diversity in the fish kingdom. We identified homolog genes of MafG and MafK but not MafF in zebrafish, indicating the former two are conserved among vertebrates. In addition, a novel type of small Maf protein MafT was identified. MafT protein bound MARE sequence as a homodimer or heterodimers with zebrafish Nrf2 or p45 Nfe2. Co-overexpression of MafT and Nrf2 synergistically activated MARE-mediated gene expression in zebrafish embryos. These results indicated that MafT is a new member of small Maf proteins and involved in the Nrf2-dependent gene regulation in cellular defense system.

Keywords: Diethylmaleate; Heterodimer; Luciferase assay; Nrf2; p45; Nfe2; Phase 2 induction; Radiation hybrid mapping; Small Maf protein; Transcription; Zebrafish

The induction of phase 2 enzyme genes is an important regulatory response for cytoprotection against electrophilic insults and reactive oxygen species [1]. Expression of phase 2 detoxifying enzymes and antioxidant proteins is strongly induced upon exposure to low levels of electrophiles or oxidative stress. Activation of the cellular defense system by phase 2 inducers renders cells more resistant to the potential challenges of a subsequent stress. This coordinated response is regulated through a *cis*-acting element called the antioxidant responsive element (ARE) or electrophile responsive element (EpRE) within the regulatory region of each gene. Analysis of gene disruption in mice has revealed that the transcription factor Nrf2 plays central roles in the ARE/EpRE-mediated transcriptional induction [2,3].

Nrf2 belongs to the family of Cap'n'collar (CNC)-type basic region-leucine zipper (bZIP) proteins, which includes p45 NF-E2, Nrf1, Nrf3, Bach1, and Bach2 [4]. Activation of Nrf2 is regulated in several steps: nuclear translocation, protein stabilization, and DNA binding [5]. Keap1, a member of the Kelch family of proteins, regulates the former two steps [6,7]. In the absence of phase 2 inducers, Nrf2 associates with Keap1 in the cytoplasm and is rapidly degraded by the ubiquitin–proteasome pathway, but upon the addition of phase 2 inducers, Nrf2 is stabilized, translocates into nuclei, and conducts the activation of target gene transcription [6,8]. Control of DNA binding is also critical for the Nrf2 functions, since Nrf2 cannot bind to the ARE/EpRE as a monomer or a homodimer, but Nrf2 must heterodimerize with one of the small Maf proteins for DNA binding and transactivation [9,10].

Seven members of Maf proteins have been identified in vertebrates, which are divided into the large and small Maf subfamilies [4]. The large Maf proteins include c-Maf [11], MafB [12], Nrl [13], and L-maf/MafA/S-maf

☆ *Abbreviations:* ARE, antioxidant responsive element; bZIP, basic region-leucine zipper; CNC, cap'n'collar; cR, centiRays; CSKN1E, casein kinase I epsilon isoform; DEM, diethylmaleate; EH, extended homology; EMSA, electrophoretic mobility shift assays; EpRE, electrophile responsive element; EST, expressed sequence tags; LFNG, lunatic fringe; LG, linkage group; MARE, Maf recognition element; RT-PCR, reverse transcriptase-polymerase chain reaction.

* Corresponding author. Fax: +81-29-847-9195.
E-mail address: kobayash@tara.tsukuba.ac.jp (M. Kobayashi).

0006-291X/$ - see front matter © 2004 Elsevier Inc. All rights reserved.
doi:10.1016/j.bbrc.2004.05.131

[14–16], which all contain an N-terminal acidic domain that serves as a transactivation domain. Rest of the members, MafF, MafG, and MafK, constitute the small Maf protein family that possesses a bZIP motif mediating the DNA binding and dimer formation in common, but lack any recognizable transcriptional effector domains [10,17]. Both large and small Maf proteins commonly recognize a specific palindromic sequence TGCTGA(C/G)TCAGCA, called MARE (Maf recognition element) [18]. Even though the small Maf proteins do not have a transactivation domain, they affect transcription either by forming heterodimers with CNC proteins [9,18–22] or homodimers that can displace active MARE binding factors [18].

MafF, MafG, and MafK were originally identified in chicken, while mammalian homologs of these were later identified in both mouse and human, suggesting that these three paralogs are conserved among vertebrates [21,23–28]. Remarkable similarities in amino acid sequences among the three small Maf proteins have led us to speculation regarding their functional redundancy. Indeed, in vitro analyses revealed that MafF, MafG, and MafK are functionally interchangeable [10,18] and transgenic overexpression of MafK proteins could compensate for the loss of MafG in gene knockout line of mice [29].

On the other hand, null mutant mice of either *mafK* or *mafF* [26,27,30] showed no apparent phenotype, while *mafG* mutant mice displayed both mild neurological and hematological phenotypes [26]. Each small Maf gene is expressed in overlapping but distinct tissue distribution pattern during development [17,26,27], which may be the reason why disruption of the single gene *mafG* showed specific phenotypes. The *mafG::mafK* compound mutants displayed far more severe phenotypes than did mutants with the *mafG* mutation alone, implying a functional redundancy of small Maf proteins and an importance of their gene dosage [31,32]. In support of the Maf dosage hypothesis, transgenic overexpression of MafK in mice severely affected T cell proliferation and function [33], and elevation not only reduction of the small Maf protein abundance caused severe defects in megakaryopoiesis [29].

Recently, we identified both Nrf2 and Keap1 in zebrafish, demonstrating that the Nrf2–Keap1 system also regulates the expression of cytoprotective genes in fish [34]. Although there has been no report for fish small Maf proteins, four members of the large Mafs have been isolated in zebrafish [16,35,36] in addition to another member of zebrafish CNC protein p45 NF-E2 [37]. These information strongly imply that small Maf proteins may also be present in fish. Therefore, it has been of interest to know whether fish has all three small Maf proteins or not. In this study, we tried to isolate small Maf proteins in zebrafish and compare their structures with those of higher vertebrates. We identified cDNAs for four small Maf proteins in zebrafish, one MafK, and two MafG homologs in addition to a novel subtype MafT, which appears to exist specifically in fish. Interestingly, we could not find a MafF homolog in zebrafish, suggesting that both MafK and MafG are conserved among vertebrates, but not MafF is conserved in fish.

Materials and methods

Isolation of cDNAs. cDNA clones encoding zebrafish small Maf proteins were prepared by reverse transcriptase-polymerase chain reaction (RT-PCR) using total RNA from zebrafish day 4 larvae and specific primers. The primers have the following sequences: *mafk*, GGGTCG ACGACAGATTTTTGAAGAGTTCTG and 5′-GGTCTAGAGAGC ATCTCAGATTCAGATTC; *mafg1*, 5′-GGGTCGACGATTCAGAC TGTCATCTTGTG and 5′-GGTCTAGAGATGAACGACCCTGTG CTTG; *mafg2*, 5′-GGGTCGACGTTTTGCAGATCTGCGTGGC and 5′-GGTCTAGACTGCAGCTCTATGGTGCAC; and *maft*, 5′-G GGGATCCATGACTTCAGACGGCAGAG and 5′-GGGTCGACA AGCCTTCCAGCTCACGC. Several independent clones for each small Maf gene were isolated and analyzed to eliminate PCR errors. For *maft*, a cDNA library of 15–19-h stage zebrafish [38] was screened using a partial cDNA fragment as a probe to isolate full-length clone. Expression of small Maf genes was analyzed by RT-PCR as described previously [34] using following primers: *mafk*, 5′-GGGGATCCGCCAT GACGACTCATTTTAAAGC and 5′-GGTCTAGACTACGATTG TGCTGAAAAGG; *mafg1*, 5′-GGGGATCCAGGTGGAGAAGCTC GCCTC and 5′-GGCTCGAGCATTATGACCGTGCTTCTG; *mafg2*, 5′-CATGACGACCACTAATAAAGG and 5′-CTACTAAGACCTG GCGTCG; *maft*, 5′-GGGGATCCATGACTTCAGACGGCAGAG and 5′-GGGTCGACAAGCCTTCCAGCTCACGC; and *ef1α*, 5′-GCC CCTGCCAATGTA and 5′-GGGCTTGCCAGGGAC.

Fish and inducer treatment. Zebrafish embryos were obtained by natural mating. For induction studies, fish were placed in culture dishes or in tanks containing 100 μM diethylmaleate (DEM).

Plasmid construction. The plasmids pCS2mafG1, pCS2HAmafG2, pCS2mafK, pCS2mafT, and pCS2nfe2 were constructed by subcloning cDNAs for the open reading frame regions of zebrafish *mafg1*, *mafg2*, *mafk*, *maft*, and *nfe2* [37], respectively, into pCS2+ vector. In the case of pCS2HAmafG2, cDNA corresponding to HA-tag (YPYDVPDYA) was inserted after initiation ATG sequence. Other plasmids used in this study (pCS2nrf2 and pRBGP2) were described previously [18,34].

Luciferase assay. Luciferase assay was performed as described previously [34] with a slight modification. Briefly, 50 pg of the circular reporter constructs was injected alone or with synthetic capped RNAs for overexpressing transcriptional factors into embryos at the one-cell stage. Embryos were harvested at midgastrula and the luciferase activity in five embryos for each condition was determined. All luciferase activities were analyzed using the Dual-Luciferase Reporter Assay System (Promega) according to the manufacturer's instruction. Injection efficiencies were routinely normalized to the activity of a *Renilla* luciferase expression plasmid, pRL-TK. At least three independent experiments, each carried out in duplicate, were performed.

Electrophoretic mobility shift assays. Proteins were prepared by in vitro transcription and translation reactions using TNT wheat germ extract (Promega). A single MARE containing oligonucleotide (5′-TCGAGCTCGGAATTGCTGACTCATCATTACTC, identical to #25 nucleotide in Kataoka et al.. [10]) was prepared by annealing synthetic oligonucleotides and ^{32}P-labeled using Rediprime II DNA Labelling System (Amersham Biosciences). Proteins were incubated with 2 fmol of ^{32}P-labeled probe at room temperature for 30 min in 20 μl of electrophoretic mobility shift assay (EMSA) binding buffer [20 mM Hepes–HCl (pH 7.6), 60 mM KCl, 4% Ficoll (4×10^5), 1 μg

poly(dI–dC), and 0.66 mM dithiothreitol]. Complexes were resolved by electrophoresis on a 4% polyacrylamide gel.

Radiation hybrid mapping. Radiation hybrid mapping using panel LN54 was performed as described in Hukriede et al. [39] using specific primers for each small Maf gene. Sequences of each primer are following: *mafk*, 5′-TTGACCAAGGAAGACGTGG and 5′-CTGTGATTGGC AGACTTGAC; *mafg1*, 5′- GAGAGCTGAATCAGCACTTG and 5′- CAGCAACTTTGCCTGGTATG; *mafg2*, 5′-CCGAGTCAAGCGCG TAACG and 5′-AGACCTGGCGTCGGTCTTG; *maft*, 5′-AGGTAC AGAAGCTGAAGCAG and 5′-CTTGACTATGGTGATGACGG; and *cskn1e*, 5′- CTCTAGCAGAACAGCTGAGG and 5′- CTCACC AGACTGAGGTACAC.

Results and discussion

Isolation of four zebrafish small Maf cDNAs

We found four candidate genes for zebrafish homologs of small Maf proteins in the zebrafish genomic DNA (http://www.ensembl.org/Danio_rerio/) and expressed sequence tag (EST) databases (http://www.ncbi.nlm.nih.gov/dbEST/index.html). Based on the sequence information, full-length cDNA clones, *mafk*, *mafg1*, *mafg2*, and *maft* (see below for assignment and naming), were isolated by RT-PCR using total RNA from Day 4 larvae or by cDNA library screening. The percentage identity of deduced amino acid sequences between zebrafish and mouse MafK [23] was 82%, and those between zebrafish MafG1 or MafG2 and mouse MafG [26] were 88% and 85%, respectively. These results indicate that both MafK and MafG are highly conserved in the fish. The high similarity between MafG1 and MafG2 (88% identity) also suggests that the *mafg* locus was duplicated in the course of fish evolution. Fig. 1A shows multiple alignments of vertebrate small Maf proteins. From this comparison, four highly conserved regions emerge among vertebrate small Maf proteins. The extended homology (EH) and basic regions that are essential for binding to the MARE sequences [10,13,40] are conserved among the large Maf proteins. On the contrary, the other two conserved amino acid stretches, N-terminal KALKVK and C-terminal SVITIVK, were characteristic for small Maf proteins, although their functions remain to be characterized.

Sequence comparison reveals the presence of new small Maf protein MafT

An important observation was that deduced amino acid sequences of the fourth clone showed relatively low homology to all mouse small Mafs (MafK 58%, MafG 54%, and MafF 57%), suggesting that this small Maf clone may belong to a novel subfamily of small Maf proteins. While we could find a gene encoding highly homologous protein to this new small Maf in the fugu genomic DNA database (83% identity, clone number M000373 in http://fugu.hgmp.mrc.ac.uk/Analysis/), we could not find such gene in mouse, human or other vertebrate databases, implying that this subfamily is specific for teleost. We therefore named this new member of small Maf protein as MafT (small Maf in Teleost). In reverse, we could find any homologous genes to MafF neither in zebrafish nor in fugu databases (data not shown). Thus, mammals and birds have only MafF, while fish has only MafT. These results allow us to speculate that these two small Maf subfamilies might be derived from the common MafF/MafT ancestor. While genetic distance of MafF and MafT was considerably far in the phylogenetic tree (Fig. 1B), it is also possible that these two subfamilies emerged independently.

Genetic mapping of zebrafish small Maf genes

We mapped zebrafish genes for four small Mafs on the linkage map by using LN54 hybrid panel [39]. Table 1 shows the results of gene mapping. Both *mafk* and *mafg1* were mapped to linkage group 3 (LG3), 388.04 and 503.01 centiRays (cR) from the most terminal markers in each linkage group, respectively. These loci are very close to the map positions of *lfng* and *axin2*, zebrafish homologs of human lunatic fringe (*LFNG*) and *AXIN2*. Since human *MAFK* and *MAFG* are localized in close proximity of *LFNG* and *AXIN2* loci as is the case for zebrafish genes, these results argue for the presence of strong synteny between zebrafish and human genes. *mafg2* was mapped to LG11, where synteny seems not to exist with human *MAFG* or other small Maf genes. The result suggests that *mafg2* is a second MafG homolog that emerges from the fish-specific evolution. *maft* is mapped on LG12 192.54 cR from the terminal, where no adjacent gene has been mapped. Importantly, we found a 194 kb length contig of fugu genomic DNA containing puffer fish homolog of MafT gene (M000373) and a homolog for epsilon isoform of human casein kinase I (CSKN1E) gene. Human *CSKN1E* localizes on 22q13.1 where *MAFF* is also localized. We isolated a partial cDNA for the zebrafish CSKN1E homolog (*cskn1e*) based on information of the EST database (DDBJ/EMBL/GenBank Accession No. CF998445) and mapped its position. As expected, *cskn1e* was mapped to the identical position with *maft* under current resolution. These results thus support our contention that MafT and MafF are derived from a common MafF/MafT ancestor, albeit their sequences are diverged significantly during the molecular evolution.

Expression profiles of small Maf mRNAs in zebrafish

It has been shown that mouse *mafF*, *mafG*, and *mafK* exhibited distinct temporal expression profiles in developing embryos [26,27]. They also show different tissue-specific expression patterns in adult mice [27,31]. In addition, the expression of small Mafs in human and

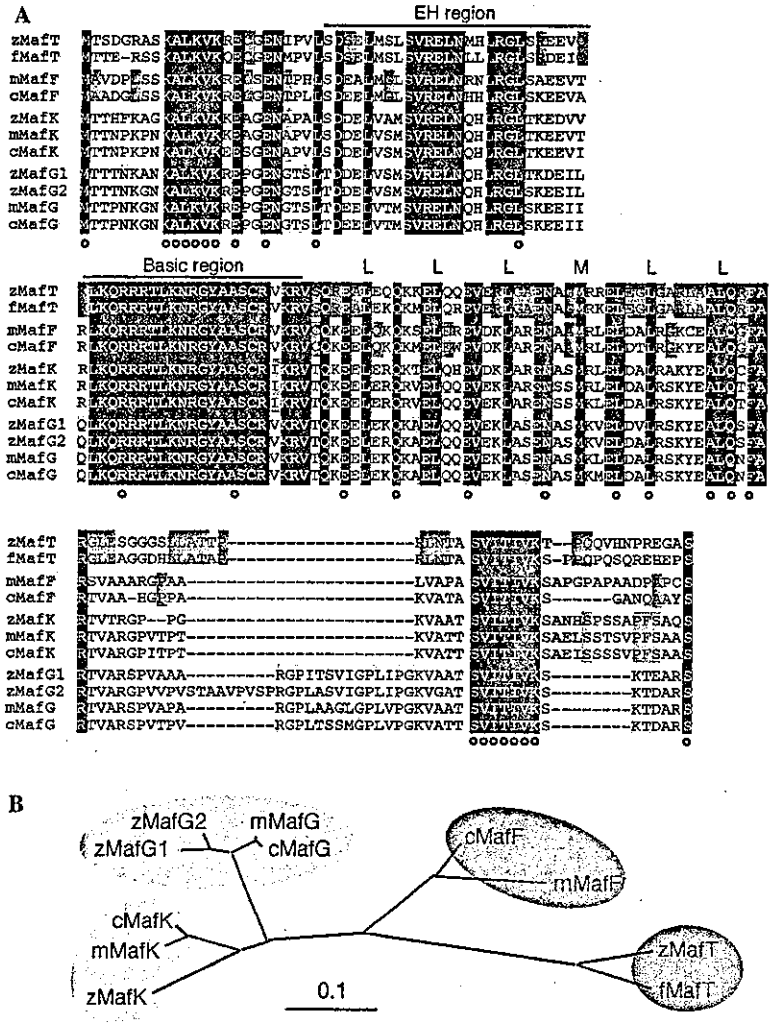

Fig. 1. Comparison of the vertebrate small Maf proteins. (A) Sequence alignment of various small Maf proteins. Conserved amino acids among all small Maf proteins are exhibited by white characters with black background, and those among only MafT, MafF, MafK, and MafG subfamilies are highlighted in purple, pink, blue and green, respectively. Amino acids highlighted in yellow indicate those conserved among MafT and MafF proteins. Open circles denote amino acids conserved among small Maf but not large Maf proteins. Heptad repeats of L or M indicate the leucine zippers. Nucleotide sequence data of *mafg1*, *mafg2*, *mafk*, and *maft* have been deposited in the DDBJ/EMBL/GenBank databases with accession numbers AB167540, AB167541, AB167542, and AB167543, respectively. (B) Phylogenetic tree of small Maf proteins. c, chicken; f, fugu; m, mouse; and z, zebrafish. Scale bar, genetic distance.

Table 1
Genetic mapping and conserved syntenies of small Maf genes

Zebrafish genes	Map positions	Human genes	Map positions
mafk	LG3-388.04 cR	*MAFK*	7p22
lfng	LG3-379.07 cR	*LFNG*	7p22
mafg1	LG3-503.01 cR	*MAFG*	17q25
axin2	LG3-501.1 cR	*AXIN2*	17q23-q24
mafg2	LG11-473.32 cR		
maft	LG12-192.54 cR	*MAFF*	22q13.1
csnk1e	LG12-192.54 cR	*CSNK1E*	22q13.1

Map positions for zebrafish *lfng* and *axin2* were cited from ZFIN Genetic Maps (http://zfin.org/cgi-bin/mapper_select.cgi), and those for human genes from NCBI human genome resources (http://www.ncbi.nlm.nih.gov/mapview/).

chicken was also demonstrated to be tissue-specific [17,21,24,25,28]. The difference in small Maf gene expression profiles led us to speculate the presence of significant variations in the regulatory mechanisms between the known small Maf genes and that of MafT. Thus, it is of interest to analyze the expression profiles of small Maf genes in zebrafish.

We therefore investigated tissue distribution of the small Maf mRNAs in adult fish. Total RNA fractions were prepared from various tissues in 7-month-old zebrafish and analyzed by RT-PCR (Fig. 2A). Amount of cDNA was standardized with the expression level of *ef1α*, a gene encoding a widely expressed translational elongation factor. While *maft* was expressed ubiquitously, its expression was relatively abundant in the

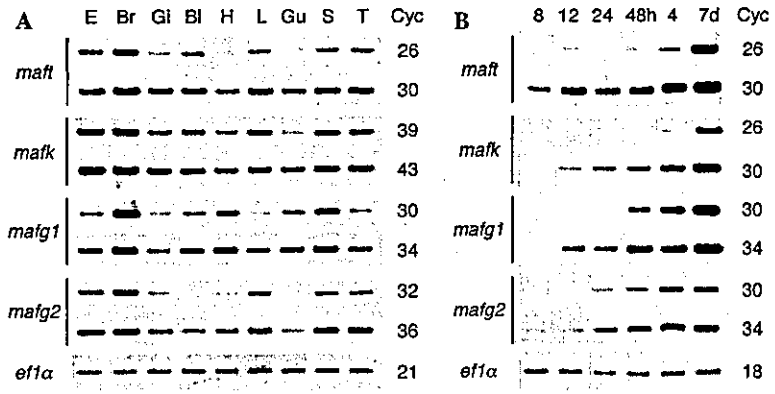

Fig. 2. Expression of small Maf mRNAs in zebrafish. Total RNA isolated from 7-month-old adult tissues (A) or whole body of embryos or larvae at the indicated developmental stages (B) was analyzed by RT-PCR using specific primers for each small Maf gene. Expression of *ef1α* was used to standardize amount of cDNA. The numbers indicate reaction cycles (Cyc) performed in the PCR. E, eye; Br, brain; Gi, gill; Bl, bladder; H, heart; L, liver; Gu, gut; S, spleen; and T, testis.

brain but scarce in the gill, heart, and gut. Expression profiles of *mafk* and *mafg2* were similar to *maft*, except a weak expression in the bladder in the case of *mafg2*. *mafg1* was also expressed ubiquitously, but of relatively high level in the heart and gut, and low level in the liver and testis in comparison with other small Maf genes.

We also examined the expression of zebrafish small Maf genes at embryonic and larval stages. RT-PCR analyses demonstrated that all Maf genes were expressed in every tested stage, but only at low level before hatching (48–72 h) during early embryogenesis (Fig. 2B).

Inducible expression of small Maf genes by DEM

In human cells or mouse tissues, the expression of small Maf genes is induced by the treatment of cells with phase 2 inducers or electrophiles [41,42]. To examine whether these inducers can also activate the expression of zebrafish small Maf genes, we analyzed expression of the small Maf genes in adult gill and whole body of larvae after treatment with DEM, a potent inducer of

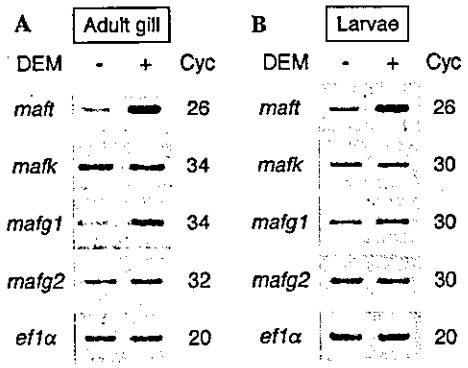

Fig. 3. Induction of small Maf genes after DEM treatment. Total RNA from adult gill (A) or whole body of larvae (B) was prepared after treatment with 100 μM DEM for 6 h and analyzed by RT-PCR using specific primers for small Maf genes.

phase 2 enzyme genes not only in mammals but also in zebrafish [34]. Fig. 3 shows that the expression of *maft* and *mafg1* was induced by the DEM treatment. This result indicates that regulatory mechanisms of small Maf genes are conserved among vertebrate. It is also consistent with the previous report, in that the induction level of each small Maf gene was varied among human cell lines [42]. While we could not find a significant difference in responsiveness to DEM between adult and larvae, *maft* in zebrafish showed highest induction level among small Maf genes. This observation shows very good agreement with that of *MAFF* in human cells [42].

Activity of MafT protein to heterodimerize with CNC proteins and bind to DNA

We then carried out to assess the ability of MafT and other zebrafish small Maf proteins forming homodimers or heterodimers with the known members of the zebrafish CNC proteins, i.e., Nrf2 and p45 Nfe2 [34,37], exploiting a single MARE containing oligonucleotide [10] as a probe (Fig. 4). Formation of homodimers was observed in the case of MafT and MafK, but it was not obvious for MafG1 nor MafG2 (Fig. 4, lanes 4, 7, 10, and 13, arrow). The weakened activity of MafG1 and MafG2 to form homodimers may be due to insolubility of homotypic full-length proteins under the conditions used for EMSA, since this was also observed when we examined mouse or chicken MafG proteins (data not shown) [10]. When we tested heterodimer formation of zebrafish small Maf proteins with CNC proteins, appearance of slower migrating bands was found upon the addition of Nrf2 to the reaction mixture (Fig. 4, closed arrowheads). These bands correspond to Nrf2-small Maf heterodimers, since specific antibodies for Nrf2 and small Mafs abolished the bands (data not shown). Similarly, an additional band to the homodimer band was observed after combining p45 Nfe2 to the reaction

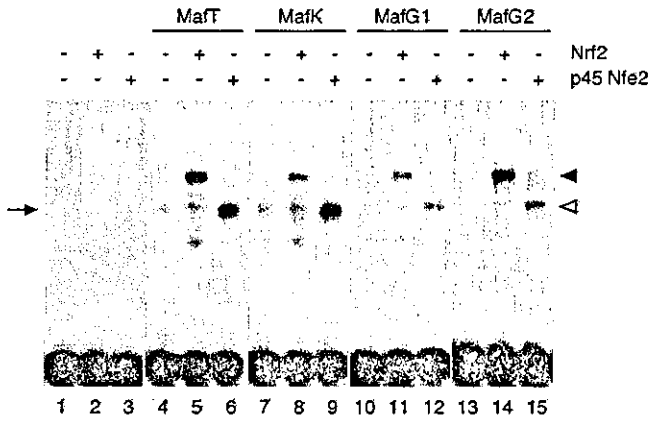

Fig. 4. DNA binding and interaction with CNC proteins of zebrafish small Maf proteins. Autoradiographic image of EMSA with the single MARE containing probe. Binding reactions were carried out with in vitro translated proteins as indicated. Arrow and arrowheads indicate complexes containing small Maf homodimers and small Maf-CNC protein heterodimers, respectively.

mixture (Fig. 4, open arrowheads). We confirmed that this additional band corresponded to the complex containing small Maf-p45 Nfe2 heterodimers by super-shift analyses using FLAG-tagged protein of p45 Nfe2 and antibodies against FLAG and small Maf proteins (data not shown). These results thus indicate that the properties of MafT are similar to those of other small Mafs.

MafT and other small Maf proteins of zebrafish enhance transactivation activity of Nrf2

MafF, MafK, and MafG have been shown to act as transcriptional repressors, when each of them was force expressed in cultured cells [10,18,23]. The repression was brought about by the lack of transactivation domains in the small Maf proteins, so that homodimers of small Maf proteins tend to inhibit binding of CNC transactivators to the MARE sequences. In order to elucidate whether MafT has any hidden transactivation domains, we analyzed transregulation activity of MafT in zebrafish embryos by reporter gene assays. To this end, luciferase gene fused to 3× MARE sequences of chicken β-globin enhancers was used as a reporter (pRBGP2) [18]. After co-injection of the reporter construct with MafT mRNA into zebrafish embryos at the one-cell stage, luciferase activity of the whole cell extract was measured at mid-gastrula. As shown in Fig. 5A, overexpression of MafT shows no increase of the luciferase activity. Similar results were obtained when amount of injecting mRNA was elevated to 50 pg (data not shown). These results thus indicate that MafT does not contain any canonical transactivation domains.

We next examined the effect of MafT on transactivation activity of Nrf2. Overexpression of Nrf2 alone strongly activated the expression of the reporter gene (Fig. 5A), as we previously described [34]. When MafT was co-expressed with Nrf2, the luciferase activity was further activated by nearly 10-fold (Fig. 5B). To elucidate whether this activity was MafT specific, we also examined the effect of MafK, MafG1, and MafG2 on the Nrf2 transactivation activity and found that all these proteins can activate the Nrf2 activity (Fig. 5C).

When amount of co-injecting MafT mRNA was increased to 250 pg, relative activity of luciferase reduced to approximately 1/15 of that in embryos injected with Nrf2 mRNA alone. The high expression level of MafT may suppress MARE-dependent transcription, probably due to forming non-transactive MafT–MafT homodimers and competing with heterodimeric transactivators' binding to MARE. These results strongly support our notion that the balance between small Maf proteins and Nrf2 or other CNC proteins determines the output of transcription [29].

Some previous reports using the culture cell-transfection systems showed that the addition of small Maf proteins provokes only repression of the Nrf2 activity

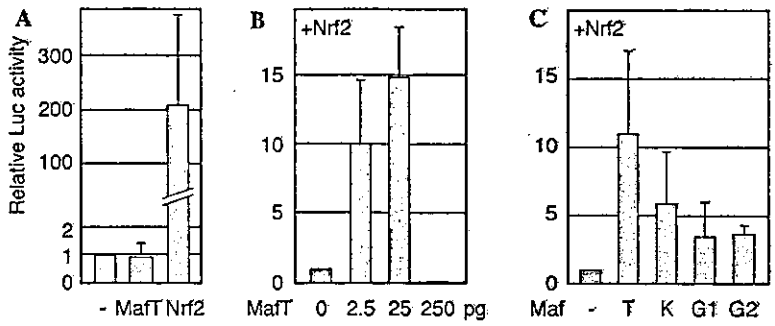

Fig. 5. MafT and other small Maf proteins enhance transactivation activity of Nrf2. (A) Fifty picograms of reporter constructs was co-injected with 12.5 pg MafT or 50 pg Nrf2 mRNAs into embryos at the one-cell stage and luciferase (Luc) activity was analyzed at midgastrula. Luciferase activity in the absence of MafT or Nrf2 (denoted as –) was set at 1. (B) Effect of co-overexpression of MafT on the Nrf2 activity. Indicated amount of MafT mRNA was co-injected with 50 pg Nrf2 mRNA and reporter constructs into zebrafish embryos. Luciferase activity in the embryos overexpressing only Nrf2 was set at 1. (C) Effect of co-overexpression of MafK, MafG1 or MafG2 on the Nrf2 activity. Five picograms each of small Maf mRNA was co-injected with 50 pg Nrf2 mRNA and reporter constructs into zebrafish embryos. The results of more than three independent experiments are shown, each carried out in duplicate. Standard deviation values are shown by bars.

[24,43–45]. In contrast, this study explicitly demonstrates the activation phase of Nrf2 activity by small Maf proteins. One plausible explanation for the difference is to assume the distinct abundance of small Maf and Nrf2 in the nucleus of culture cells and zebrafish embryos. Whereas small Maf proteins translocate quickly into the nucleus [4], Nrf2 localizes in cytoplasm with binding to Keap1 [6,7] and is degraded rapidly by proteasome [8] without stimuli of electrophiles. Thus, the expression level of small Maf proteins in nuclei of conventional culture cells may be relatively abundant compared to Nrf2, so that further addition of small Mafs to the cells does not activate the reporter gene transcription. In contrast, in early zebrafish embryos the expression level of all small Maf proteins is quite low compared with later stages (see Fig. 2B). Therefore, the expression of small Maf proteins effectively supplied partner molecules for Nrf2 and the effect of small Mafs was detectable. The experimental system utilizing the zebrafish embryos thus provides an excellent model system to assess the transregulatory activity of small Maf proteins in vivo. Zebrafish system provides a powerful tool for the analysis of gene regulation, such as external fertilization, transparent embryos, and application of random mutagenesis and screening techniques. New aspects of Maf and CNC proteins may emerge from future zebrafish analyses.

Concluding remarks

In this report, we identified MafT as a new member of small Maf proteins. This study also suggests that small Maf proteins are important intrinsic partners for Nrf2. Among many other questions still unanswered, the following question is intriguing as to why does fish develop its original subtype MafT? Searching for small Maf genes in the fugu genomic DNA database demonstrates that fugu also has MafG and MafK in addition to MafT, but not MafF, suggesting the conservation of MafG and MafK, but not MafF and MafT among the vertebrate (data not shown). As the mouse *mafF* gene is strongly expressed in the lung, a tissue which fish does not have [27], one simple hypothesis is that MafT was specialized for water-living organism. However, expression of zebrafish *maft* in the gill or bladder was relatively weak compared to those of other tissues. Thus, the question remains to be elucidated.

Acknowledgments

We thank Yuko Nakayama for technical assistance in radiation hybrid mapping, Toshiko Arai, Masami Doi, Masami Eguchi, Toyoko Kinoshita, Yoshie Terashita, and Yoshiko Wada for help in fish maintenance, and Hitoshi Osanai and Miki Takeuchi for help and discussion. We are grateful to Tetsuro Ishii for advice and helpful comments, Marc Ekker for LN54 hybrid panel, Leonard Zon for p45 Nfe2, Bruce Appel for cDNA library, and Hozumi Motohashi and Ken Itoh for critical reading of the manuscript. This work was supported by Grants-in-Aid from the Japan Society for Promotion of Sciences (JSPS-RFTF), the Japan Science and Technology Corporation (ERATO), and the Ministry of Education, Science, Sports and Culture of Japan.

References

[1] K. Itoh, T. Ishii, N. Wakabayashi, M. Yamamoto, Regulatory mechanisms of cellular response to oxidative stress, Free Radic. Res. 31 (1999) 319–324.
[2] K. Itoh, T. Chiba, S. Takahashi, T. Ishii, K. Igarashi, Y. Katoh, T. Oyake, N. Hayashi, K. Satoh, I. Hatayama, M. Yamamoto, Y. Nabeshima, An Nrf2/small Maf heterodimer mediates the induction of phase II detoxifying enzyme genes through antioxidant response elements, Biochem. Biophys. Res. Commun. 236 (1997) 313–322.
[3] T. Ishii, K. Itoh, S. Takahashi, H. Sato, T. Yanagawa, Y. Katoh, S. Bannai, M. Yamamoto, Transcription factor Nrf2 coordinately regulates a group of oxidative stress-inducible genes in macrophages, J. Biol. Chem. 275 (2000) 16023–16029.
[4] H. Motohashi, T. O'Connor, F. Katsuoka, J.D. Engel, M. Yamamoto, Integration and diversity of the regulatory network composed of Maf and CNC families of transcription factors, Gene 294 (2002) 1–12.
[5] M. Kobayashi, M. Yamamoto, Molecular mechanisms activating the Nrf2–Keap1 pathway of antioxidant gene regulation, Antioxid. Redox Signal. (in press).
[6] K. Itoh, N. Wakabayashi, Y. Katoh, T. Ishii, K. Igarashi, J.D. Engel, M. Yamamoto, Keap1 represses nuclear activation of antioxidant responsive elements by Nrf2 through binding to the amino-terminal Neh2 domain, Genes Dev. 13 (1999) 76–86.
[7] N. Wakabayashi, K. Itoh, J. Wakabayashi, H. Motohashi, S. Noda, S. Takahashi, S. Imakado, T. Kotsuji, F. Otsuka, D.R. Roop, T. Harada, J.D. Engel, M. Yamamoto, Keap1-null mutation leads to postnatal lethality due to constitutive Nrf2 activation, Nat. Genet. 35 (2003) 238–245.
[8] K. Itoh, N. Wakabayashi, Y. Katoh, T. Ishii, T. O'Connor, M. Yamamoto, Keap1 regulates both cytoplasmic-nuclear shuttling and degradation of Nrf2 in response to electrophiles, Genes Cells 8 (2003) 379–391.
[9] K. Itoh, K. Igarashi, N. Hayashi, M. Nishizawa, M. Yamamoto, Cloning and characterization of a novel erythroid cell-derived CNC family transcription factor heterodimerizing with the small Maf family proteins, Mol. Cell. Biol. 15 (1995) 4184–4193.
[10] K. Kataoka, K. Igarashi, K. Itoh, K.T. Fujiwara, M. Noda, M. Yamamoto, M. Nishizawa, Small Maf proteins heterodimerize with Fos and may act as competitive repressors of the NF-E2 transcription factor, Mol. Cell. Biol. 15 (1995) 2180–2190.
[11] K. Kataoka, M. Nishizawa, S. Kawai, Structure–function analysis of the maf oncogene product, a member of the b-Zip protein family, J. Virol. 67 (1993) 2133–2141.
[12] K. Kataoka, K.T. Fujiwara, M. Noda, M. Nishizawa, MafB, a new Maf family transcription activator that can associate with Maf and Fos but not with Jun, Mol. Cell. Biol. 14 (1994) 7581–7591.
[13] A. Swaroop, J. Xu, H. Pawar, A. Jackson, C. Skolnick, N. Agarwal, A conserved retina-specific gene encodes a basic motif/leucine zipper domain, Proc. Natl. Acad. Sci. USA 89 (1992) 266–270.
[14] H. Ogino, K. Yasuda, Induction of lens differentiation by activation of a bZIP transcription factor, L-Maf, Science 280 (1998) 115–118.

[15] S. Benkhelifa, S. Provot, O. Lecoq, C. Pouponnot, G. Calothy, M.-P. Felder-Schmittbuhl, mafA, a novel member of the maf proto-oncogene family, displays developmental regulation and mitogenic capacity in avian neuroretina cells, Oncogene 17 (1998) 247–254.
[16] M. Kajihara, S. Kawauchi, M. Kobayashi, H. Ogino, S. Takahashi, K. Yasuda, Isolation, characterization, and expression analysis of zebrafish large Mafs, J. Biochem. 129 (2001) 139–146.
[17] K.T. Fujiwara, K. Kataoka, M. Nishizawa, Two new members of the maf oncogene family, mafK and mafF, encode nuclear b-Zip proteins lacking putative trans-activator domain, Oncogene 8 (1993) 2371–2380.
[18] K. Igarashi, K. Kataoka, K. Itoh, N. Hayashi, M. Nishizawa, M. Yamamoto, Regulation of transcription by dimerization of erythroid factor NF-E2 p45 with small Maf proteins, Nature 367 (1994) 568–572.
[19] Ø. Johnsen, N. Skammelsrud, L. Luna, M. Nishizawa, H. Prydz, A.-B. Kolsto, Small Maf proteins interact with the human transcription factor TCF11/Nrf1/LCR-F1, Nucleic Acids Res. 24 (1996) 4289–4297.
[20] T. Oyake, K. Itoh, H. Motohashi, N. Hayashi, H. Hoshino, M. Nishizawa, M. Yamamoto, K. Igarashi, Bach proteins belong to a novel family of BTB-basic leucine zipper transcription factors that interact with MafK and regulate transcription through the NF-E2 site, Mol. Cell. Biol. 16 (1996) 6083–6095.
[21] M.G. Marini, K. Chan, L. Casula, Y.W. Kan, A. Cao, P. Moi, hMAF, a small human transcription factor that heterodimerizes specifically with Nrf1 and Nrf2, J. Biol. Chem. 272 (1997) 16490–16497.
[22] A. Kobayashi, E. Ito, T. Toki, K. Kogame, S. Takahashi, K. Igarashi, N. Hayashi, M. Yamamoto, Molecular cloning and functional characterization of a new Cap'n'collar family transcription factor Nrf3, J. Biol. Chem. 274 (1999) 6443–6452.
[23] K. Igarashi, K. Itoh, H. Motohashi, N. Hayashi, Y. Matuzaki, H. Nakauchi, M. Nishizawa, M. Yamamoto, Activity and expression of murine small Maf family protein MafK, J. Biol. Chem. 270 (1995) 7615–7624.
[24] T. Toki, J. Itoh, J. Kitazawa, K. Arai, K. Hatakeyama, J. Akasaka, K. Igarashi, N. Nomura, M. Yokoyama, M. Yamamoto, E. Ito, Human small Maf proteins form heterodimers with CNC family transcription factors and recognize the NF-E2 motif, Oncogene 14 (1997) 1901–1910.
[25] V. Blank, M.J. Kim, N.C. Andrews, Human MafG is a functional partner for p45 NF-E2 in activating globin gene expression, Blood 89 (1997) 3925–3935.
[26] J.A. Shavit, H. Motohashi, K. Onodera, J. Akasaka, M. Yamamoto, J.D. Engel, Impaired megakaryopoiesis and behavioral defects in mafG-null mutant mice, Genes Dev. 12 (1998) 2164–2174.
[27] K. Onodera, J.A. Shavit, H. Motohashi, F. Katsuoka, J. Akasaka, J.D. Engel, M. Yamamoto, Characterization of the murine mafF gene, J. Biol. Chem. 274 (1999) 21162–21169.
[28] T. Kimura, R. Ivell, W. Rust, Y. Mizumoto, K. Ogita, C. Kusui, Y. Matsumura, C. Azuma, Y. Murata, Molecular cloning of a human MafF homologue, which specifically binds to the oxytocin receptor gene in term myometrium, Biochem. Biophys. Res. Commun. 264 (1999) 86–92.
[29] H. Motohashi, F. Katsuoka, J.A. Shavit, J.D. Engel, M. Yamamoto, Positive or negative MARE-dependent transcriptional regulation is determined by the abundance of small Maf proteins, Cell 103 (2000) 865–875.
[30] K.J. Kotkow, S.H. Orkin, Complexity of the erythroid transcription factor NF-E2 as revealed by gene targeting of the mouse p18 NF-E2 locus, Proc. Natl. Acad. Sci. USA 93 (1996) 3514–3518.
[31] K. Onodera, J.A. Shavit, H. Motohashi, M. Yamamoto, J.D. Engel, Perinatal synthetic lethality and hematopoietic defects in compound mafG::mafK mutant mice, EMBO J. 19 (2000) 1335–1345.
[32] F. Katsuoka, H. Motohashi, Y. Tamagawa, S. Kure, K. Igarashi, J.D. Engel, M. Yamamoto, Small Maf compound mutants display central nervous system neuronal degeneration, aberrant transcription, and Bach protein mislocalization coincident with myoclonus and abnormal startle response, Mol. Cell. Biol. 23 (2003) 1163–1174.
[33] K. Yoh, T. Sugawara, H. Motohashi, Y. Takahama, A. Koyama, M. Yamamoto, S. Takahashi, Transgenic over-expression of MafK suppresses T cell proliferation and function in vivo, Genes Cells 6 (2001) 1055–1066.
[34] M. Kobayashi, K. Itoh, T. Suzuki, H. Osanai, K. Nishikawa, Y. Katoh, Y. Takagi, M. Yamamoto, Identification of the interactive interface and phylogenic conservation of the Nrf2–Keap1 system, Genes Cells 7 (2002) 807–820.
[35] C.B. Moens, S.P. Cordes, M.W. Giorgianni, G.S. Barsh, C.B. Kimmel, Equivalence in the genetic control of hindbrain segmentation in fish and mouse, Development 125 (1998) 381–391.
[36] M. Schvarzstein, A. Kirn, P. Haffter, S.P. Cordes, Expression of Zkrml2, a homologue of the Krml1/val segmentation gene, during embryonic patterning of the zebrafish (*Danio rerio*), Mech. Dev. 80 (1999) 223–226.
[37] S.J. Pratt, A. Drejer, H. Foott, B. Barut, A. Brownlie, J. Postlethwait, Y. Kato, M. Yamamoto, L.I. Zon, Isolation and characterization of zebrafish NFE2, Physiol. Genomics 11 (2002) 91–98.
[38] B. Appel, J.S. Eisen, Regulation of neuronal specification in the zebrafish spinal cord by Delta function, Development 125 (1998) 371–380.
[39] N.A. Hukriede, L. Joly, M. Tsang, J. Miles, P. Tellis, J.A. Epstein, W.B. Barbazuk, F.N. Li, B. Paw, J.H. Postlethwait, T.J. Hudson, L.I. Zon, J.D. McPherson, M. Chevrette, I.B. Dawid, S.L. Johnson, M. Ekker, Radiation hybrid mapping of the zebrafish genome, Proc. Natl. Acad. Sci. USA 96 (1999) 9745–9750.
[40] H. Kusunoki, H. Motohashi, F. Katsuoka, A. Morohashi, M. Yamamoto, T. Tanaka, Solution structure of the DNA-binding domain of MafG, Nat. Struct. Biol. 9 (2002) 252–256.
[41] A.C. Wild, H.R. Moinova, R.T. Mulcahy, Regulation of gamma-glutamylcysteine synthetase subunit gene expression by the transcription factor Nrf2, J. Biol. Chem. 274 (1999) 33627–33636.
[42] J.A. Moran, E.L. Dahl, R.T. Mulcahy, Differential induction of mafF, mafG and mafK expression by electrophile-response-element activators, Biochem. J. 361 (2002) 371–377.
[43] T. Nguyen, H.C. Huang, C.B. Pickett, Transcriptional regulation of the antioxidant response element. Activation by Nrf2 and repression by MafK, J. Biol. Chem. 275 (2000) 15466–15473.
[44] S. Dhakshinamoorthy, A.K. Jaiswal, Small maf (MafG and MafK) proteins negatively regulate antioxidant response element-mediated expression and antioxidant induction of the NAD(P)H:Quinone oxidoreductase1 gene, J. Biol. Chem. 275 (2000) 40134–40141.
[45] J. Alam, D. Stewart, C. Touchard, S. Boinapally, A.M.E. Choi, J.L. Cook, Nrf2, a Cap'n'Collar transcription factor, regulates induction of the heme oxygenase-1 gene, J. Biol. Chem. 274 (1999) 26071–26078.

MOLECULAR AND CELLULAR BIOLOGY, Aug. 2004, p. 7130–7139 Vol. 24, No. 16
0270-7306/04/$08.00+0 DOI: 10.1128/MCB.24.16.7130–7139.2004

Oxidative Stress Sensor Keap1 Functions as an Adaptor for Cul3-Based E3 Ligase To Regulate Proteasomal Degradation of Nrf2

Akira Kobayashi,[1,2,3] Moon-Il Kang,[1,2,3] Hiromi Okawa,[1,2,3] Makiko Ohtsuji,[1,2,3] Yukari Zenke,[4] Tomoki Chiba,[5] Kazuhiko Igarashi,[4] and Masayuki Yamamoto[1,2,3]*

Center for Tsukuba Advanced Research Alliance,[1] Institute of Basic Medical Sciences,[2] and JST-ERATO Environmental Response Project,[3] University of Tsukuba, Tsukuba 305-8575, Department of Biomedical Chemistry and Leukemia Program Project, Hiroshima University Graduate School of Biomedical Sciences, Hiroshima 734-8551,[4] and Department of Molecular Oncology, Tokyo Metropolitan Institute of Medical Science, Bunkyo-Ku, Tokyo 113-8613,[5] Japan

Received 29 April 2004/Accepted 20 May 2004

Transcription factor Nrf2 is a major regulator of genes encoding phase 2 detoxifying enzymes and antioxidant stress proteins in response to electrophilic agents and oxidative stress. In the absence of such stimuli, Nrf2 is inactive owing to its cytoplasmic retention by Keap1 and rapid degradation through the proteasome system. We examined the contribution of Keap1 to the rapid turnover of Nrf2 (half-life of less than 20 min) and found that a direct association between Keap1 and Nrf2 is required for Nrf2 degradation. In a series of domain function analyses of Keap1, we found that both the BTB and intervening-region (IVR) domains are crucial for Nrf2 degradation, implying that these two domains act to recruit ubiquitin-proteasome factors. Indeed, Cullin 3 (Cul3), a subunit of the E3 ligase complex, was found to interact specifically with Keap1 in vivo. Keap1 associates with the N-terminal region of Cul3 through the IVR domain and promotes the ubiquitination of Nrf2 in cooperation with the Cul3-Roc1 complex. These results thus provide solid evidence that Keap1 functions as an adaptor of Cul3-based E3 ligase. To our knowledge, Nrf2 and Keap1 are the first reported mammalian substrate and adaptor, respectively, of the Cul3-based E3 ligase system.

Biological responses to toxic environmental stresses are regulated by several coordinated functions of cellular factors, providing animals with a means of cellular protection. The cellular factors usually involve a component that senses a stress and transmits the information as a cellular signal to transcription factors. Transcription factors then induce or regulate the expression of genes encoding cytoprotective enzymes and proteins (16, 23). It has been shown that repression of stress-responsive transcription factors is crucial for the maintenance of cellular homeostasis. This repression is especially important for avoiding unnecessary gene activation in the absence of stress stimuli. Several prototype mechanisms of such inhibitory action have been identified. For instance, von Hippel-Lindau protein (pVHL) acts as a repressor of transcription factor Hif-1α by accelerating protein degradation under conditions of normoxia (23). pVHL works to ubiquitinate Hif-1α, leading to degradation of the protein in a proteasome-dependent manner. The transcriptional activity of Hif-1α is thus repressed during normoxia (11).

Oxidative and xenobiotic stresses are known to cause many diseases, such as cancer, diabetes, and arteriosclerosis. Recent progress in this field has provided solid evidence for the contention that these stresses are sensed by the Nrf2-Keap1 system, which in response achieves cytoprotection by regulating the expression of phase 2 drug-metabolizing enzymes and antioxidant response proteins (6, 10, 16). In the absence of stress stimuli, the cytoplasmic protein Keap1 binds Nrf2 and prevents its translocation to the nucleus (10). This cytoplasmic sequestration of Nrf2 requires at least two cysteine residues in the intervening region (IVR) of Keap1. In experiments conducted in vitro, four cysteine residues in the IVR appeared to be modified by electrophiles (3, 14, 27), suggesting that Keap1 functions as a sensor for oxidative and xenobiotic stimuli through these cysteines.

Extensive studies have been executed to elucidate the molecular mechanisms governing Nrf2 activity. These studies revealed that Nrf2 is degraded rapidly by the ubiquitin-proteasome pathway (9, 15, 17, 25, 31). The rapid turnover of Nrf2 was reproducible throughout these studies and proven in vivo in experiments with a gene-manipulated mouse (9). However, the molecular mechanisms regarding Nrf2 degradation are still controversial. One group reported that ubiquitination of Nrf2 is carried out in a Keap1-independent manner, whereas another group claimed Keap1-dependent degradation of Nrf2 (15, 31). We also found that Nrf2 is degraded through two distinct pathways: a proteasome-dependent rapid turnover and a relatively slow turnover in the nucleus (9).

The ubiquitin-dependent proteolysis system regulates the abundance of proteins and serves a central regulatory function in many biological processes, including cell cycle progression, signal transduction, and transcription (7). Ubiquitin conjugation to substrate proteins is carried out by the sequential reaction of three enzymes (19): the ubiquitin-activating enzymes (E1), the ubiquitin-conjugating enzymes (E2), and the ubiquitin ligases (E3). E3 ligases provide two distinct functions; one is to target substrate protein, and the other is to catalyze isopeptide bond formation between the substrate protein and ubiquitin.

* Corresponding author. Mailing address: Center for TARA, University of Tsukuba, 1-1-1 Tennoudai, Tsukuba, 305-8575, Japan. Phone: 81-29-853-6158. Fax: 81-29-853-7318. E-mail: masi@tara.tsukuba.ac.jp.

It has been shown that there are several types of E3 ligase. Cullin (Cul)-based E3 ligases regulate the turnover of important transcription factors and are composed of several subunits. Cul is a scaffold protein in the E3 ligase complex and forms a catalytic core complex with Roc1/Rbx1/Hrt1, with Roc1 recruiting a cognate E2 enzyme. Six Cul protein members have been identified in mammals: Cul1, Cul2, Cul3, Cul4A, Cul4B, and Cul5 (29). To target substrate proteins specifically, the Cul-Roc1 complex requires an adaptor molecule. Cul1 preferentially binds the adaptor molecules Skp1 and F-box protein, while Cul2 binds pVHL and elongin C. These complexes are referred to as the SCF (Skp1–Cul1–F-box) and ECS (elongin-Cul2-SOCS) E3 ligases, respectively. Recently, in *Caenorhabditis elegans* and *Schizosaccharomyces pombe*, a subset of proteins containing a BTB domain was reported to function as a distinct group of substrate-specific adaptors which preferentially bind to Cul3. The BTB proteins seem to target certain substrates into the E3 ligase complex by virtue of their protein-interaction domains, the Kelch motifs and MATH domain (4, 5, 21, 30). However, a specific substrate for the mammalian Cul3 system has not yet been identified.

Two distinct molecular mechanisms for the contribution of Keap1 to the rapid turnover of Nrf2 have been assumed (9). Keap1 may contribute to the turnover of Nrf2 by merely retaining Nrf2 in the cytoplasm such that Nrf2 is kept in close proximity to the proteasome system. Alternatively, Keap1 may promote Nrf2 degradation more effectively through the active recruitment of E3 ligase and proteasome subunits. To examine which case is actually operating, we established a system that analyzes Nrf2 degradation in vivo. This paper describes the molecular mechanisms of Nrf2 degradation involving the ubiquitin-proteasome system. Our results provide conclusive evidence that Keap1 is a stress sensor protein that functions directly as an adaptor molecule in the Cul3-based E3 ligase system in the rapid degradation of Nrf2. Thus, Keap1 plays essential roles in the Nrf2-Keap1 stress response system, not only as a sensor of oxidative and electrophilic stresses but also as a regulator of Nrf2 degradation.

MATERIALS AND METHODS

Chemical reagents. MG132 and the calpain inhibitor E64 were purchased from Peptide Institute Inc. Clasto-lactacystin β-lactone was from Calbiochem.

Plasmid construction. Cul1, Cul2, Cul4A, and Cul5 cDNAs were cloned by reverse transcription-PCR using mouse brain and testis cDNAs and inserted into the Asp718 and XhoI sites of pcDNA3-Myc (Invitrogen). Cul3 cDNA was cloned by similar reverse transcription-PCR and inserted into the EcoRI and XbaI sites of p3XFLAG-CMV-10 (Sigma). Primers used for the amplification are available on request. pCMVNrf2ΔETGE was generated by substituting the KpnI-EcoRV fragment of pCMVmNrf2 with two pieces of PCR fragments digested with KpnI and EcoRI and with EcoRI and EcoRV, respectively. pCMVNrfaΔC and pCMVNrfaΔC/ETGE were constructed by inserting the XbaI linker (amber mutation) into the blunt-ended HindIII sites of pCMVNrf2 and pCMVNrf2ΔETGE, respectively. Expression plasmids of Cul3 deletion mutants, p3Xflag Cul3N280 and p3Xflag Cul3 ΔN280, were generated by inserting PCR products into the EcoRI and XbaI sites of p3XFLAG-CMV-10 (Sigma). Primers used for the amplification are available on request. Keap1 deletion mutants and Cys mutants in the IVR were generated as described previously (12, 27). All constructs were verified by sequencing.

Cell culture and transfection. Cos7 cells and 293T cells were cultured in Dulbecco modified Eagle medium (Sigma) supplemented with 10% fetal calf serum (Gibco), 4500 mg of glucose per liter, 40 μg of streptomycin per ml, and 40 U of penicillin per ml. The DNA transfection was performed with Fugen6 (Roche) and Lipofectamine Plus (Invitrogen).

Turnover of Nrf2 in the presence of Keap1 and mutants. Full-length Keap1 or Keap1 mutants were expressed in Cos7 cells along with enhanced green fluorescent protein (EGFP). At 36 h after transfection, the cells were treated with cyclohexamide (final concentration, 10 μM) to stop de novo protein synthesis and harvested by scraping. The cells were boiled in Laemmli sample buffer supplemented with β-mercaptoethanol (final concentration, 2%) (Wako Chemicals) at several time points, as described in the legend to Fig. 1. Cell extracts were subjected to immunoblot analysis with an anti-Nrf2 antibody (C4) against the C-terminal end of Nrf2 and anti-EGFP antibody (Santa Cruz). Experiments were performed twice in duplicate.

Immunohistochemical staining. Cos7 cells expressing Nrf2 and deletion mutants were grown on cultured dishes. At 36 h after transfection, the cells were fixed with 4% paraformaldehyde and acetone, blocked with 2% goat serum and 5% skim milk for 1 h, and incubated with an anti-Nrf2 antibody (100-fold dilution). The cells were incubated with anti-rabbit antibody conjugated with fluorescein isothiocyanate (100-fold dilution) (Zymed) and washed with phosphate-buffered saline. Nuclei were stained with 4′,6-diamidino-2-phenylindole (DAPI). The cells were visualized by fluorescence microscopy (Leica DMIRB).

In vivo ubiquitination assay. 293T cells were transfected with several combinations of plasmids as described in the legend to Fig. 6, along with His-tagged Ub vector (26). At 24 h following transfection, the cells were treated with MG132 (final concentration, 2 μM) for 12 h to inhibit the proteasome function. Whole-cell extracts were prepared in lysis buffer I (20 mM Tris-HCl [pH 7.5], 0.5 M NaCl, 8 M urea, 5 mM imidazole) and incubated overnight with Ni^{2+} affinity beads (Probond resin; Invitrogen). After being washed three times with lysis buffer, the beads were boiled in the sample buffer and the eluate was subjected to immunoblot analysis with an anti-Nrf2 antibody recognizing the Neh2 domain.

Immunoprecipitation. To determine the interaction of endogenous Keap1 with Cul3 in culture cells, an immunoprecipitation experiment using anti-Keap1 antibody was performed. Whole-cell extracts of 293T cells were prepared in lysis buffer II (10 mM Tris-HCl [pH 7.5], 150 mM NaCl, 1 mM EDTA, 1 mM dithiothreitol, 0.1% Nonidet P-40, protease inhibitor cocktail [Roche Diagnostic], 10 μM MG132) and treated overnight with anti-Keap1 antibody against the N-terminal peptide (12). Immunocomplexes were precipitated with protein G (Pierce), washed three times with lysis buffer II, and subjected to immunoblot analysis using anti-Cul3 antibody (Santa Cruz), the ABC kit (Vector Laboratory), and the ECL kit (Amersham).

To analyze the interaction between Keap1 and several Cul proteins, expression plasmids for these factors were transfected into 293T cells by using Lipofectamine Plus. At 36 h after transfection, cytoplasmic extracts were prepared in buffer A (10 mM HEPES-KOH [pH 7.9], 10 mM KCl, 0.1 mM EDTA, 1 mM $MgCl_2$, 0.5 mM dithiothreitol, protease inhibitor cocktail), and NaCl was added to a final concentration of 70 mM. Cell extracts were incubated with anti-Flag M2 beads (Sigma) by generous rocking at 4°C for 4 h. The immunocomplexes were washed three times with buffer (10 mM Tris-HCl [pH 7.5], 100 mM NaCl, 0.1 mM EDTA, 1 mM $MgCl_2$, 0.1% Nonidet P-40) and subjected to immunoblot analysis with anti-Myc, anti-HA (Santa Cruz), and anti-Keap1 antibodies, separately.

RESULTS

Degradation of Nrf2 requires association with Keap1. To examine the contribution of Keap1, we established a system enabling analysis of the mechanisms involved in Nrf2 degradation. In this system, Nrf2 was transiently expressed in Cos7 cells by transfection in the presence or absence of Keap1, and a whole-cell extract was prepared to determine the stability of Nrf2 by immunoblot analysis with an anti-Nrf2 antibody. As shown in Fig. 1A, Nrf2 accumulated in Cos7 cells after transfection (lanes 1 and 2). The accumulation of Nrf2 was augmented by the addition of a proteasome inhibitor, MG132 (lane 3), indicating that Nrf2 is otherwise rapidly degraded through the proteasome pathway. Important observations are that coexpression of Keap1 significantly reduced the amounts of Nrf2 (lanes 4, 6, and 8) and that this Keap1-dependent reduction of Nrf2 was inhibited by the addition of MG132 (lanes 5, 7, and 9).

We also challenged a couple of other protease inhibitors. Of

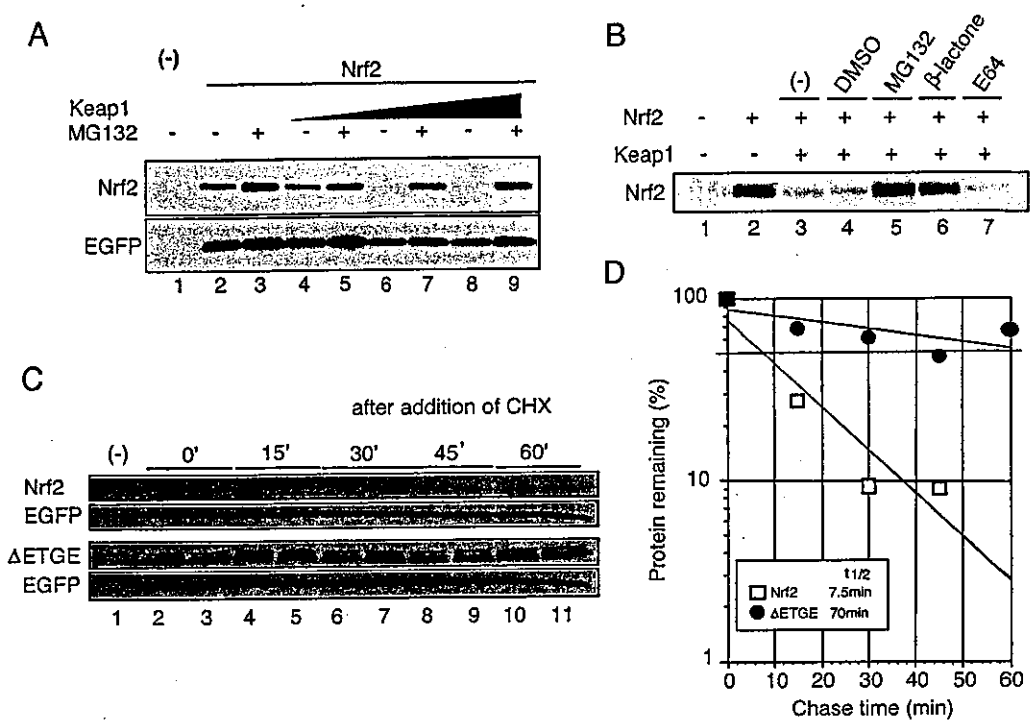

FIG. 1. Assay system to examine the degradation mechanism of Nrf2. (A) Keap1 promotes Nrf2 degradation in the in vivo degradation system. An Nrf2 expression vector (2 μg) was transfected into Cos7 cells (90% confluent) with or without the Keap1 expression vector (1.5 μg). At 24 h after transfection, the cells were treated with dimethyl sulfoxide (DMSO) (lanes 1, 2, 4, 6, and 8) and 2 μM MG132 (lanes 3, 5, 7, and 9) for 12 h and directly lysed in sodium dodecyl sulfate sample buffer. (Upper panel) Whole-cell extracts were subjected to immunoblot analysis with an anti-Nrf2 antibody. (Lower panel). The expression level of cotransfected EGFP was used as an internal control. (B) Proteasome-specific inhibitors stabilize the Nrf2 protein. Transfected cells were treated with DMSO (lane 4), 2 μM MG132 (lane 5), 2 μM clasto-lactacystin β-lactone (lane 6), and E64 (lane 7) for 12 h. Immunoblot analysis was performed as described above. (C and D) The Nrf2 expressed in this system was rapidly degraded in a Keap1-dependent manner. Nrf2 and ΔETGE mutant were transfected into cells along with Keap1. At 36 h after transfection, the cells were treated with 10 μM cycloheximide (CHX) per ml for the periods indicated. (Upper panel) Whole-cell extracts were subjected to immunoblot analysis with an anti-Nrf2 antibody. (Lower panel). The expression level of EGFP was used as an internal control. The averages of the relative band intensities of Nrf2 (open squares) and ΔETGE mutant (closed circles) represent two independent experiments performed in duplicate.

the protease inhibitors, *clasto*-lactacystin β-lactone (β-lactone) is known to be more specific to the proteasome pathway than MG132 whereas E64 is a specific inhibitor of calpain proteases. As shown in Fig. 1B, degradation of Nrf2 was inhibited by β-lactone and MG132 but not by E64 (lanes 5 to 7). These results indicate that Nrf2 is degraded in this Cos7 system in a proteasome-dependent manner.

To further examine how closely this system recapitulates the endogenous Nrf2 degradation machinery, we determined the half-life of Nrf2 in this system and compared it with that of endogenous Nrf2 (Fig. 1C and D). The half-life of Nrf2 was determined by cotransfecting Nrf2 and Keap1 expression plasmids into Cos7 cells and then treating them with cycloheximide for specific periods to inhibit de novo protein synthesis. Whole-cell extracts were then prepared from these cells and subjected to immunoblot analysis. The half-life of Nrf2 was determined to be 7.5 min in the present Cos7 system (Fig. 1D). This is in very good agreement with the half-life of 18.5 min determined for endogenous Nrf2 in our previous analysis using peritoneal macrophages (9).

The ETGE motif of Nrf2 is indispensable in the association of Nrf2 with Keap1 (13); therefore, our ETGE deletion mutant will not interact with Keap1 (data not shown). Thus, we would expect significant stabilization of this Nrf2 mutant if Keap1 is truly involved in the active degradation of Nrf2 in vivo. We measured the half-life of the ΔETGE mutant of Nrf2 and found that it was indeed stabilized markedly (Fig. 1D, $t_{1/2}$ = 70 min). These results thus demonstrate that Nrf2 is degraded in a Keap1-dependent manner in this system. Collectively, these data support our contention that the present degradation system of Nrf2 mimics the endogenous degradation of Nrf2 fairly well.

Keap1 directly promotes degradation of Nrf2. To address the question whether Keap1 actively contributes to the rapid degradation of Nrf2, we measured the turnover of Nrf2 localized exclusively in the cytoplasm. To this end, we generated two deletion mutants of Nrf2. One is a ΔC mutant, which lacks the C-terminal region including the nuclear localization signal, while the other is a ΔC/ETGE mutant, which lacks the ETGE motif as well as the C-terminal region (Fig. 2A, ΔC and ΔC/ETGE, respectively). Keap1 associated with the ΔC mutant, but not with the ΔC/ETGE mutant (data not shown). Importantly, immunohistochemical analysis showed that both mutants were localized in the cytoplasm, even in the absence of Keap1 (Fig. 2B).

Exploiting the Cos7 system, we again examined the half-life

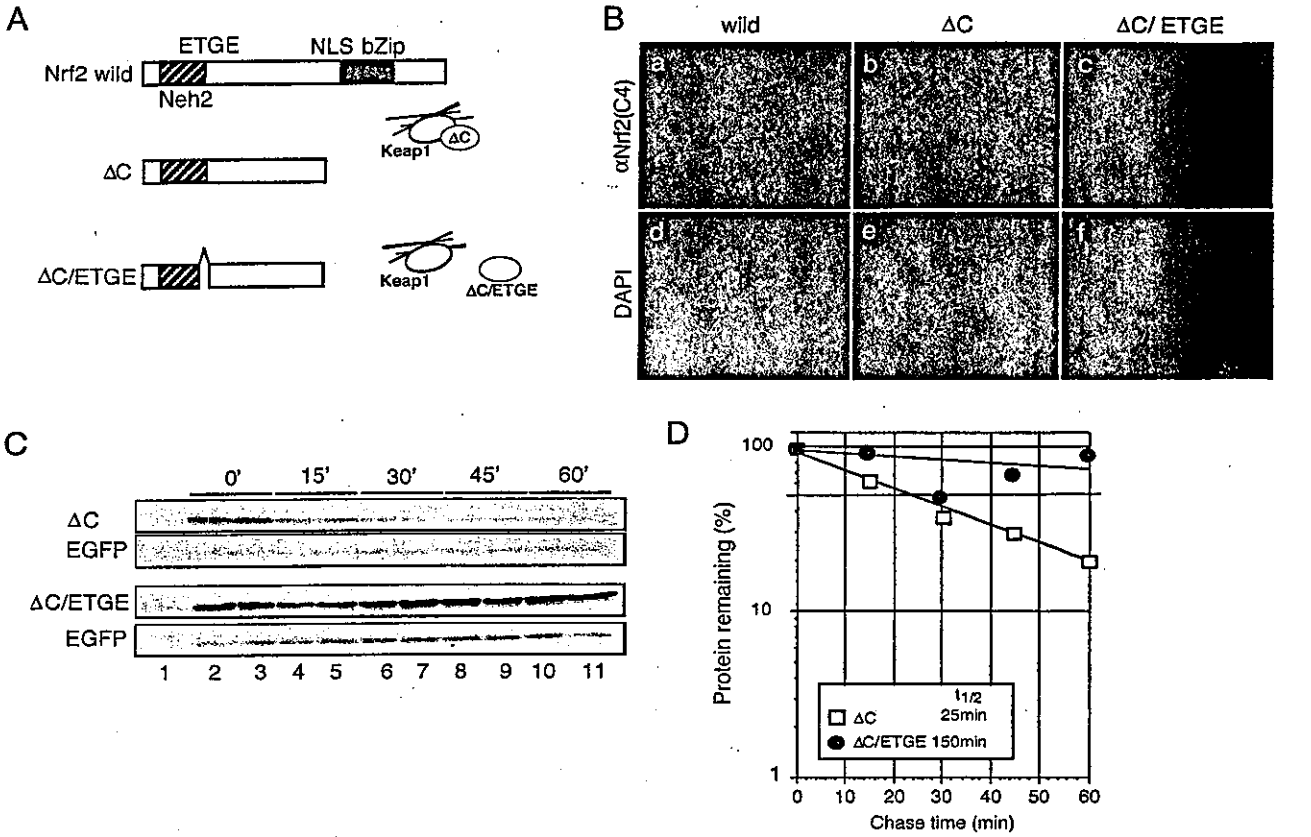

FIG. 2. Rapid turnover of Nrf2 requires its association with Keap1. (A) Schematic presentation of Nrf2 deletion mutants. ΔC lacks the C terminus including the NLS of wild-type Nrf2. ΔC/ETGE lacks both this C terminus and the ETGE motif, which is crucial for association with Keap1. (B) Cytoplasmic localization of ΔC and ΔC/ETGE mutants in Cos7 cells (b and c). These mutant proteins were stained by an immunohistochemical method with anti-Nrf2 (C4) antibody. Nuclei were stained with DAPI (d to f). (C and D) Deletion of the ETGE motif abolished the degradation of Nrf2 by Keap1. This suggests that Keap1 positively regulates the degradation of Nrf2 through its association. The experimental procedure was described in the legend to Fig. 1. The averages of the band intensities of ΔC and ΔC/ETGE mutants represent two independent experiments done in duplicate.

of Nrf2. The hypothesis behind this study is that if rapid degradation of Nrf2 requires a physical interaction with Keap1, the ΔC mutant should degrade more rapidly than the ΔC/ETGE mutant. After cotransfection of expression plasmids of these Nrf2 mutants and Keap1 into Cos7 cells, the cells were treated with cycloheximide for 36 h and harvested at several time points (Fig. 2C and D). We determined the half-life of these Nrf2 mutants by normalizing the amount of Nrf2 protein with that of coexpressed EGFP. Deletion of the C-terminal region slightly stabilized Nrf2 ($t_{1/2}$ = 25 min) compared to full-length Nrf2. In contrast, simultaneous deletion of the ETGE motif with the C-terminal region significantly stabilized Nrf2 ($t_{1/2}$ = 150 min). These data suggest that Keap1 actively promotes Nrf2 degradation whereas the mere presence of Nrf2 in the cytoplasm does not lead to its active degradation.

BTB and IVR domains of Keap1 contribute to the Nrf2 degradation. The next important study was to decipher the molecular mechanisms of how Keap1 regulates Nrf2 degradation. We executed a series of domain functional analyses of Keap1 to identify the domains in Keap1 crucial for Nrf2 degradation. Keap1 consists mainly of the BTB/POZ, IVR, and DGR domains (Fig. 3A). We therefore expressed deletion mutants of each of these domains in Cos7 cells together with Nrf2 and monitored the stability of Nrf2 by immunoblot analysis using whole-cell extracts (Fig. 3B). Deletion of the DGR domain completely abolished the Nrf2 degradation activity of Keap1 since the DGR domain is essential for the association of Keap1 with Nrf2 (lane 6). Surprisingly, deletion of either the BTB or IVR domain also impaired the Keap1 activity that leads to Nrf2 degradation (lanes 4 and 5). The expression levels of the deletion mutants were verified to be comparable by immunoblot analysis using anti-Keap1 antibodies (Fig. 3C). The BTB and IVR domain mutants could interact with Nrf2 and localize the Nrf2 reporter protein (Neh2-GFP) exclusively in the cytoplasm (12). Taken together, these results suggest that Keap1 promotes Nrf2 degradation through interaction between certain regulatory factors with the BTB or IVR domain.

Keap1 associates with Cul3 in vivo. To identify regulatory factors associated with the degradation property of Keap1, we performed several rounds of yeast two-hybrid screens using full-length Keap1 or the BTB domain as bait. However, in spite of these extensive analyses, we could not isolate factors regulating Nrf2 degradation (data not shown). Switching to a candidate approach showed that a subset of BTB proteins function as an adaptor for the Cul3-type E3 ligase complex (4, 5, 21, 30).